

Dust and Volatile Environment of the Moon

Paul Hayne

LASP / U. Colorado Boulder

Dust, Atmosphere, and Plasma Workshop 2023
Boulder, Colorado



Introduction

The dusty surface layer is the “skin” that records external processes shaping the lunar surface on timescales from hours to eons



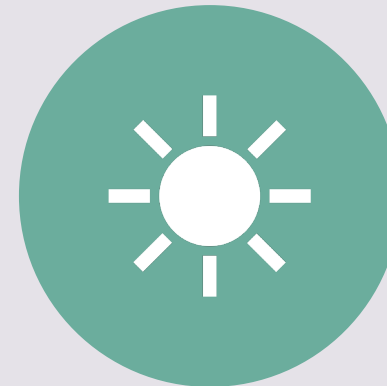
Motivation: Connecting Dust and Volatiles



IMPACTS FRAGMENT AND
PULVERIZE LUNAR CRUST,
PRODUCING REGOLITH AND FINES



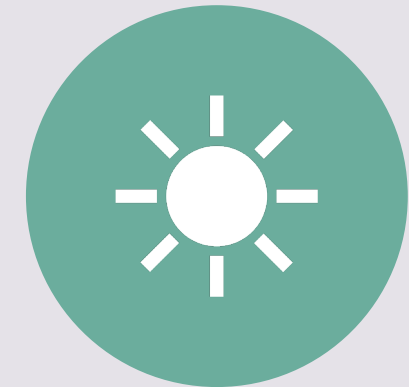
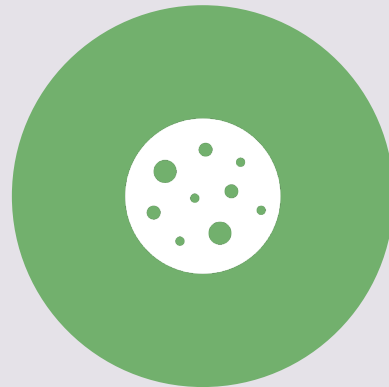
WATER AND OTHER **VOLATILES**
DELIVERED BY COMETS AND
METEORITES



SPACE WEATHERING CHANGES
SURFACE COMPOSITION AND
SUNLIGHT PHOTOLYZES AND
DESORBS WATER



Motivation: Connecting Dust and Volatiles



How do the processes involving production and transport of dust and volatiles interact on a vast range of timescales?



Billions of years

100 Myr

1 Myr

100 kyr

Timescales

hours



Outline

- Background: Apollo-era view of regolith and volatiles
- New views from NASA's Lunar Reconnaissance Orbiter and LCROSS
- Global regolith properties from Diviner
- The epiregolith and lunar eclipse observations
- Abundance and distribution of volatiles at the poles
- The young age of lunar water
- Micro cold traps
- Revisiting timescales and dust-volatile interactions



The Apollo Era View

1. Regolith



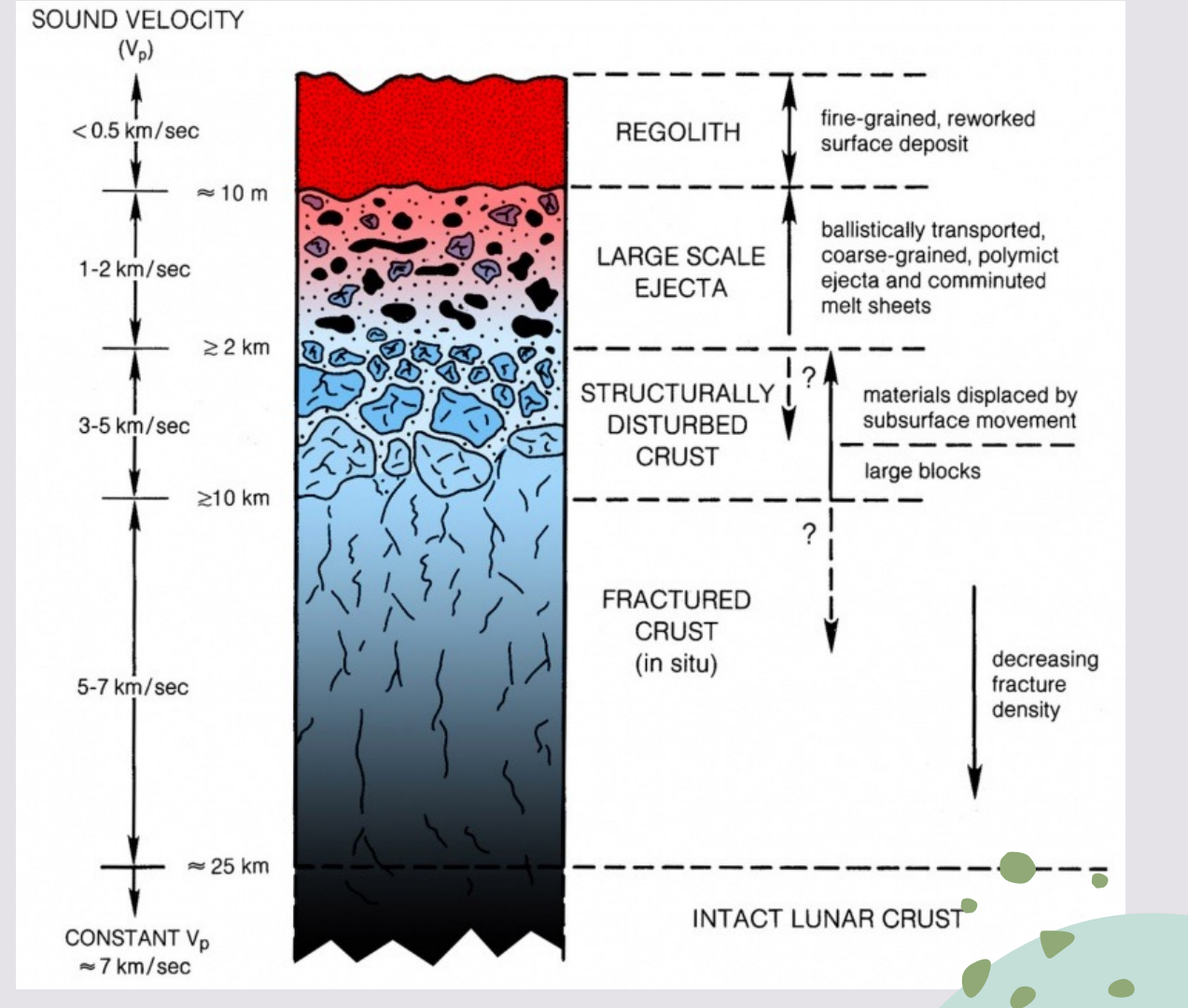
Canonical View of Regolith

Intact bedrock fractured and fragmented over time

Impact ejecta blanket the surface

Micrometeorites continuously pulverize and fragment rocks

Fines are globally redistributed



Regolith Formation Models

Gault et al. (1974) regolith gardening model calculates probability of overturn at each depth, after a certain period of time

$$\log(N) \sim -\log(\text{depth})$$

→ Expect exponential increase in density w/ depth if 'overturn' decreases density

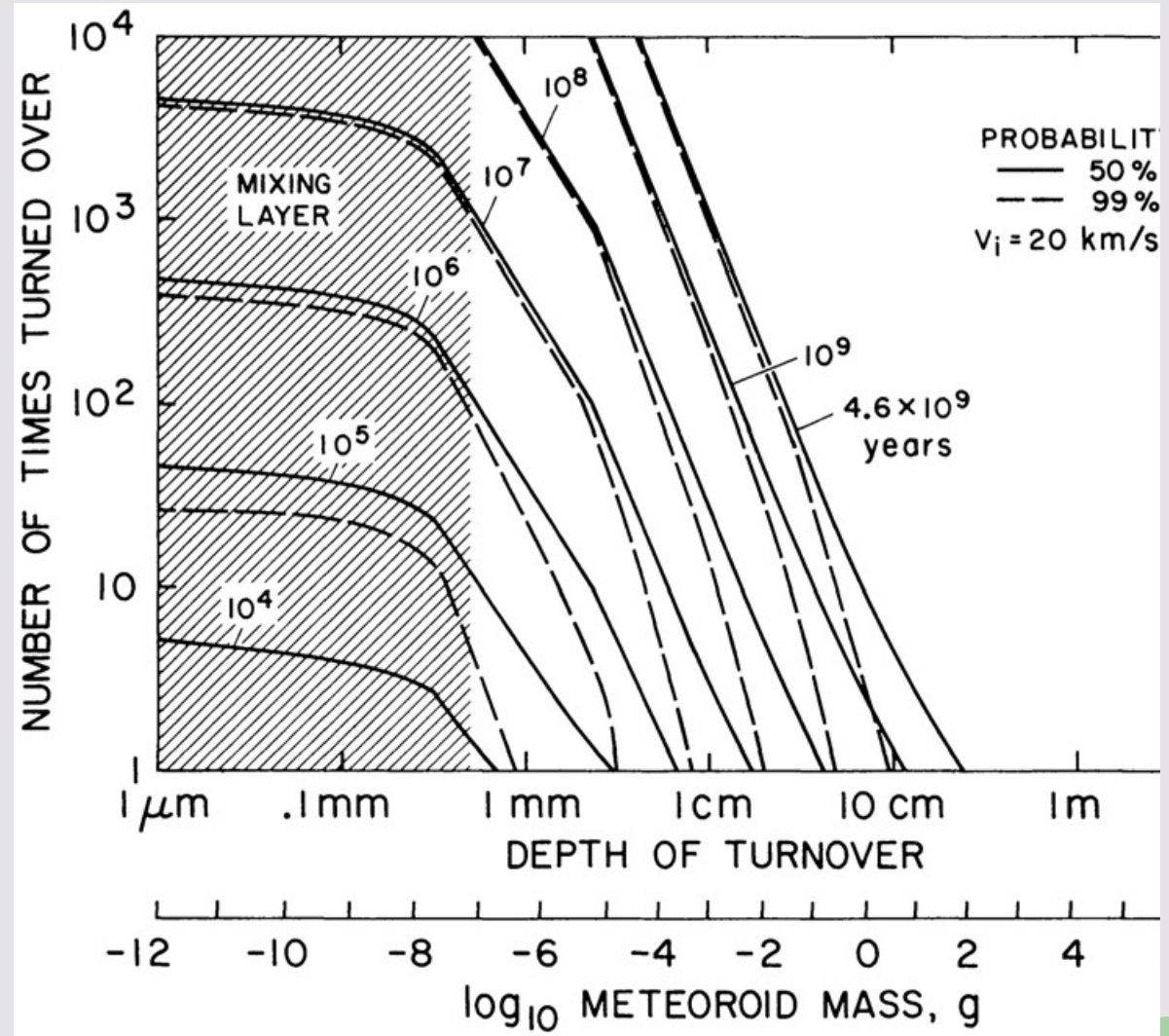


Fig. 9. Number of times n the regolith is turned over as a function of turnover depth and meteoroid mass, flux constant.

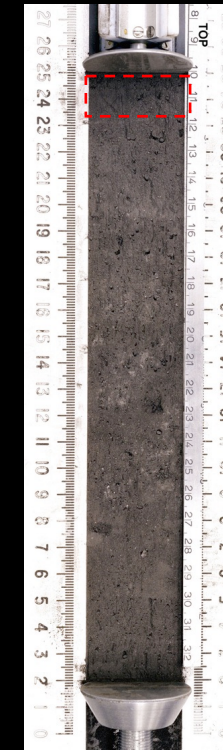
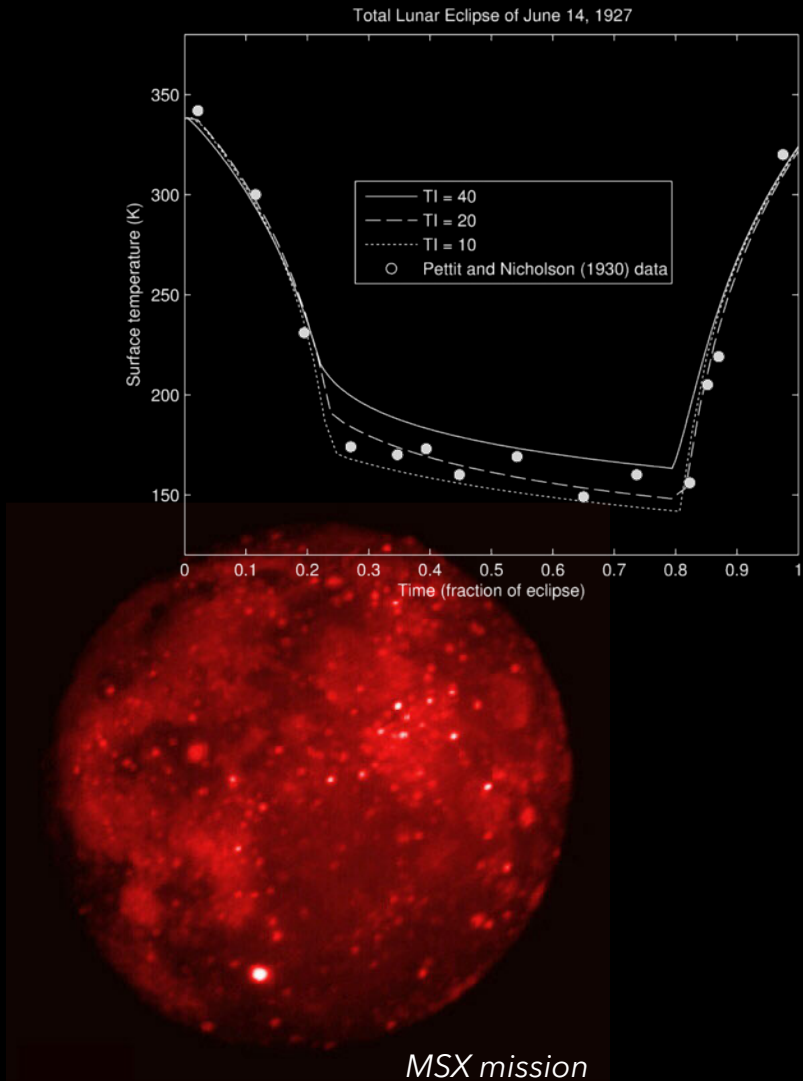
Thermal Observations of the Moon

Pettit and Nicholson (1930): first thermal IR observations of Moon, 8 to 14 μm window

Surface materials comparable to silica aerogel ($\text{T.I.} \sim 10 \text{ J m}^{-2} \text{ K}^{-1} \text{ s}^{-1/2}$)

Apollo measurements (Langseth et al., 1976) showed upper $\sim 1\text{-cm}$ layer has $\text{T.I.} \sim 10x$ lower than 1-m average
→ impact gardening

Surface roughness dominates IR emission phase function (Smith, 1967)



NASA



The Apollo Era View

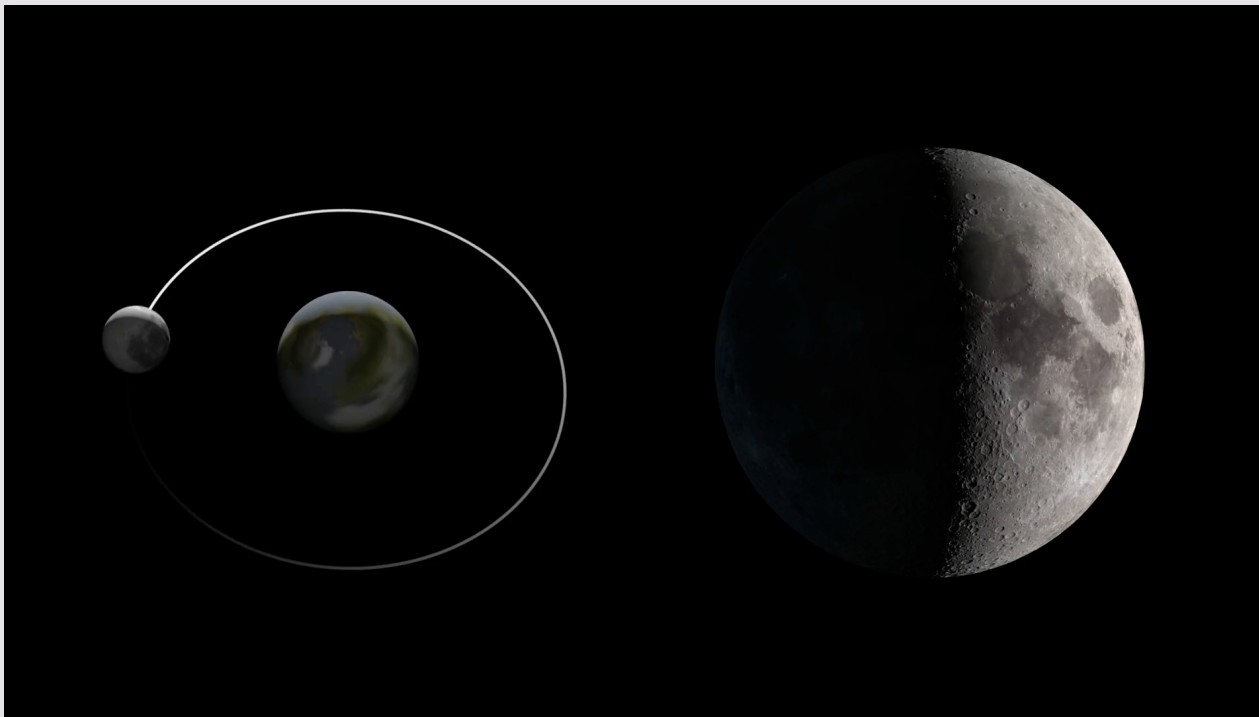
2. Volatiles

The Exospheric Cold-trapping Paradigm

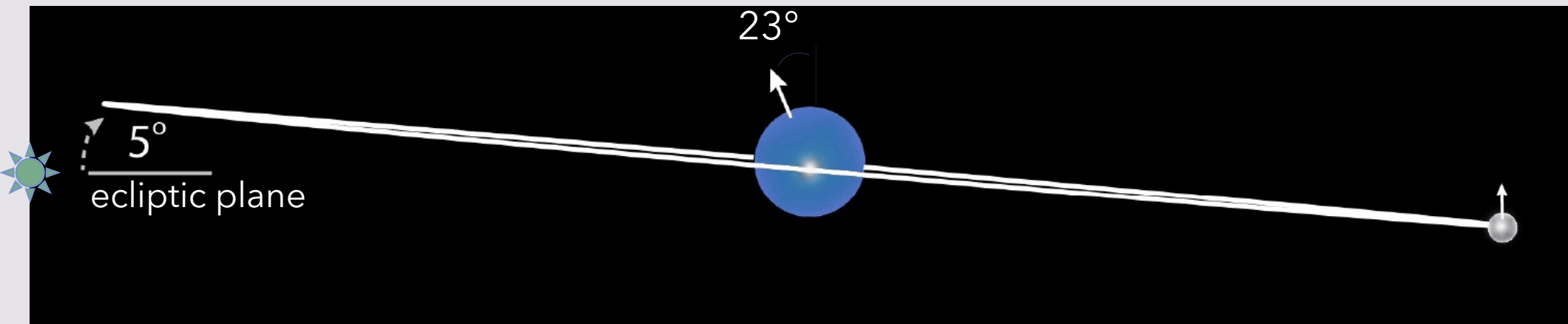
Existence of “permanently shadowed regions” (PSRs) first noted by Robert Goddard in the 1920’s

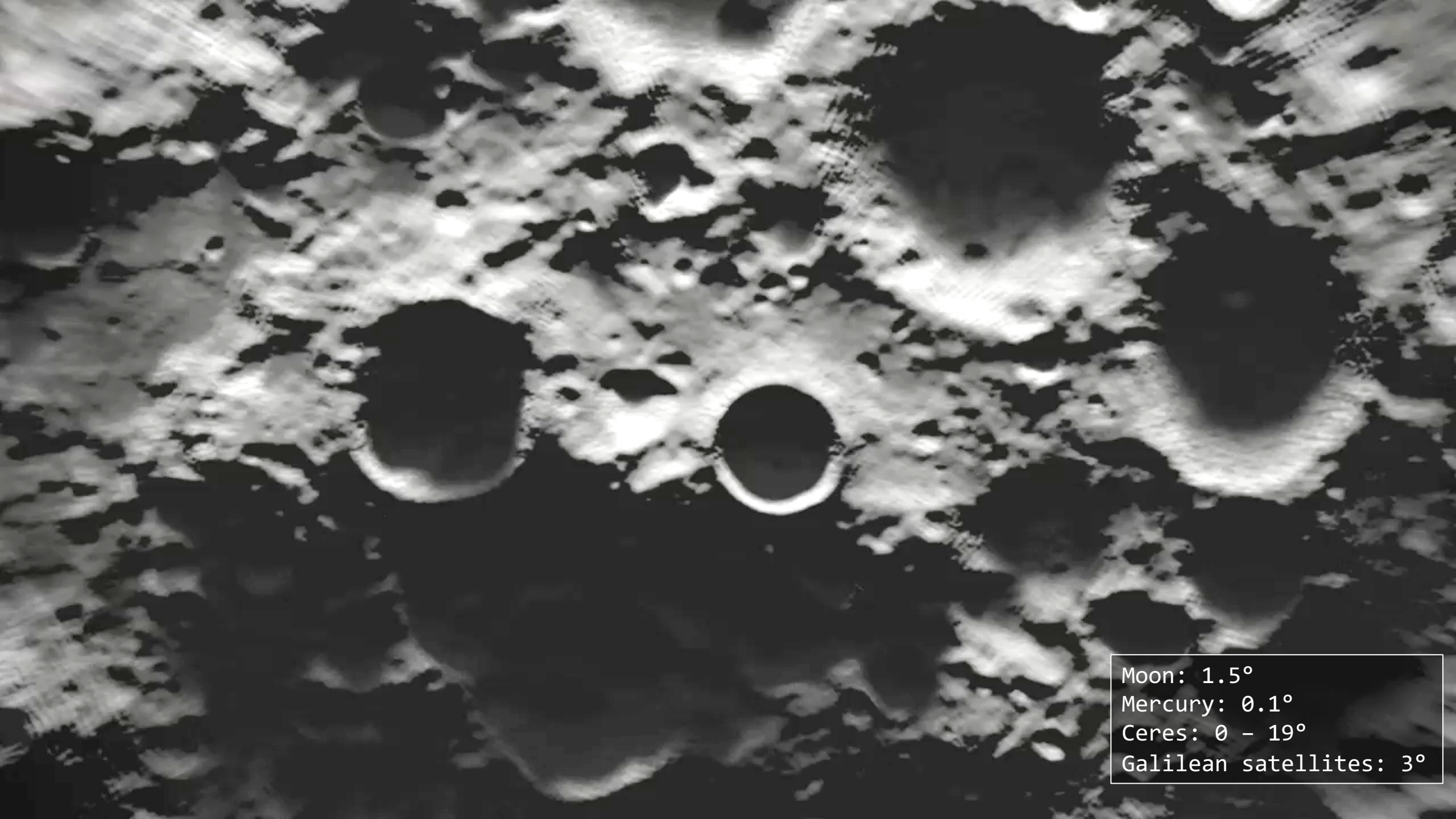
In a 1961 study, Ken Watson, Bruce Murray and Harrison Brown at Caltech worked out the possible cold-trapping mechanism for exospheric water in the PSRs

Lunar Orbital Geometry creates PSRs



The Moon's 'Special' Orbit

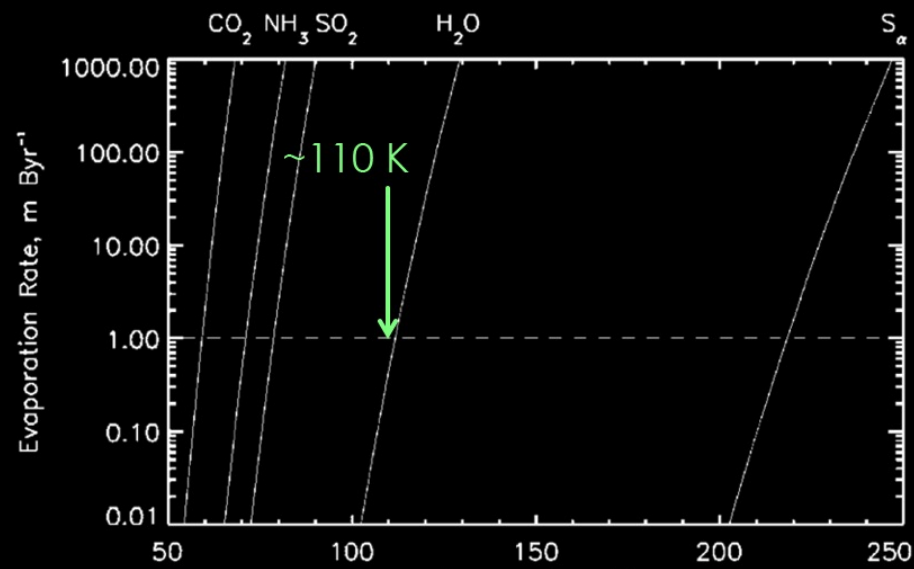
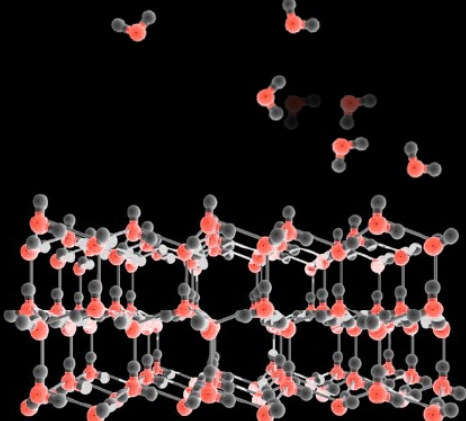




Moon: 1.5°
Mercury: 0.1°
Ceres: 0 - 19°
Galilean satellites: 3°

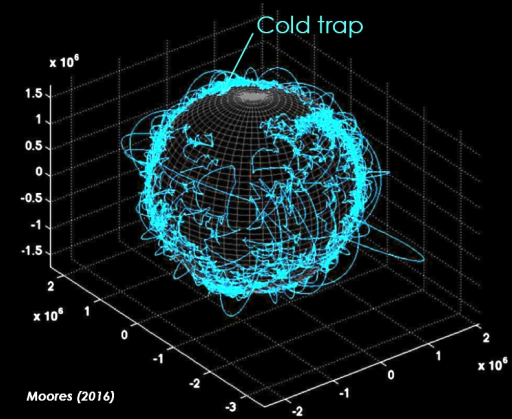
Water Stability and Cold-trapping Mechanism

$$\dot{E} = \frac{p_v(T) - p}{\sqrt{2\pi RT}}$$

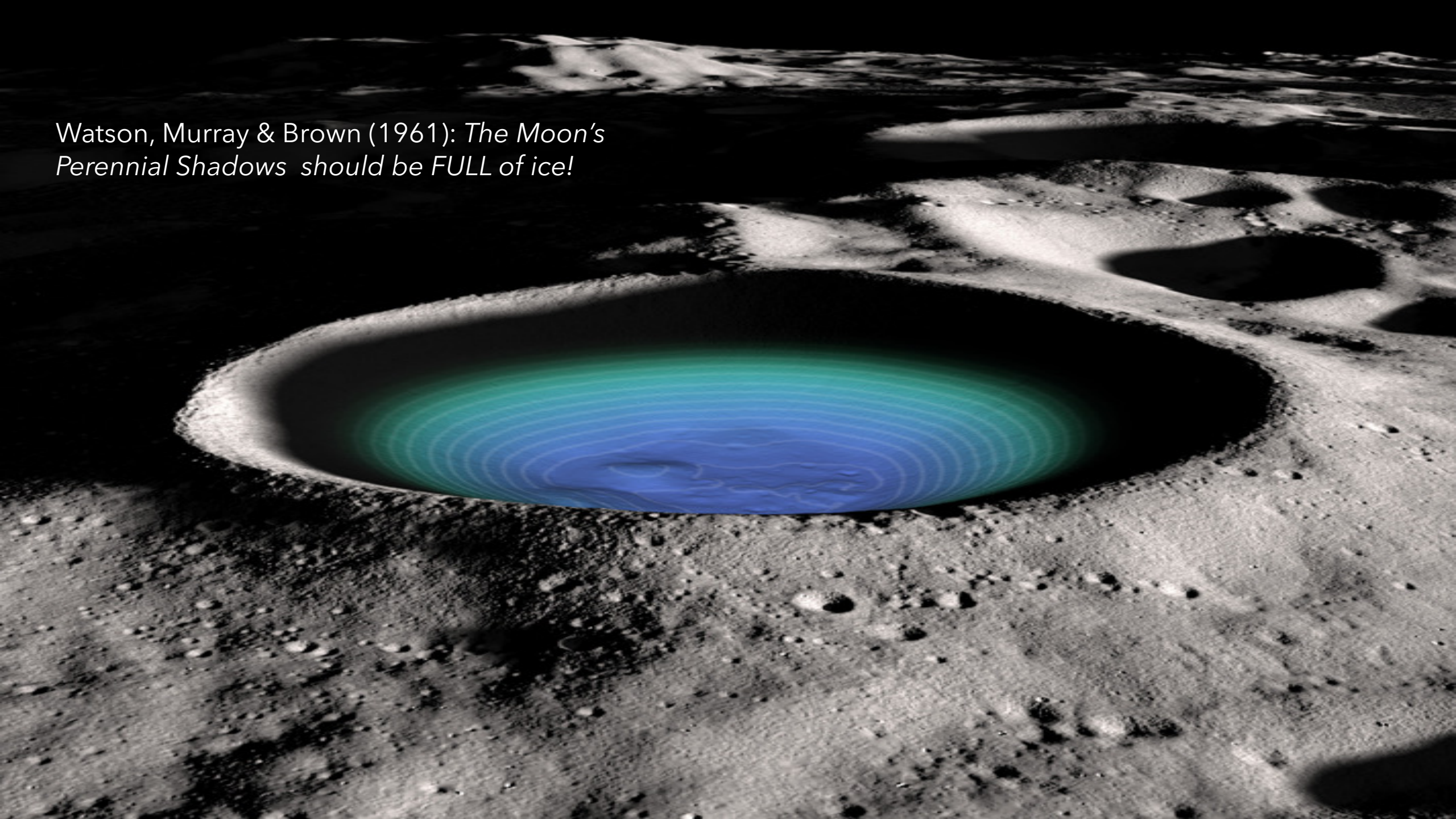


Vasavada et al., 1999

At temperatures < 110 K, water behaves "like a rock"; sublimation rate < 1 m/Gyr



Photodissociation lifetime ~hours to days
Water molecules allowed to make ~100 hops before being destroyed or cold-trapped



Watson, Murray & Brown (1961): *The Moon's Perennial Shadows should be FULL of ice!*



New Views from the Lunar Reconnaissance Orbiter Era

1. Regolith and dust



LCROSS:
Objective: Search for ice
using artificial impact

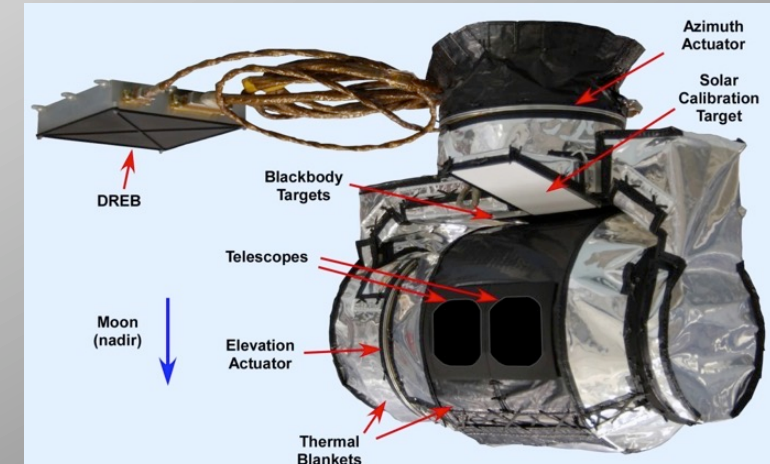
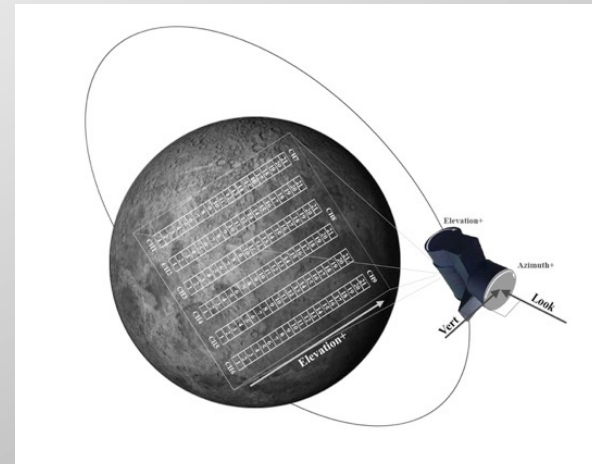
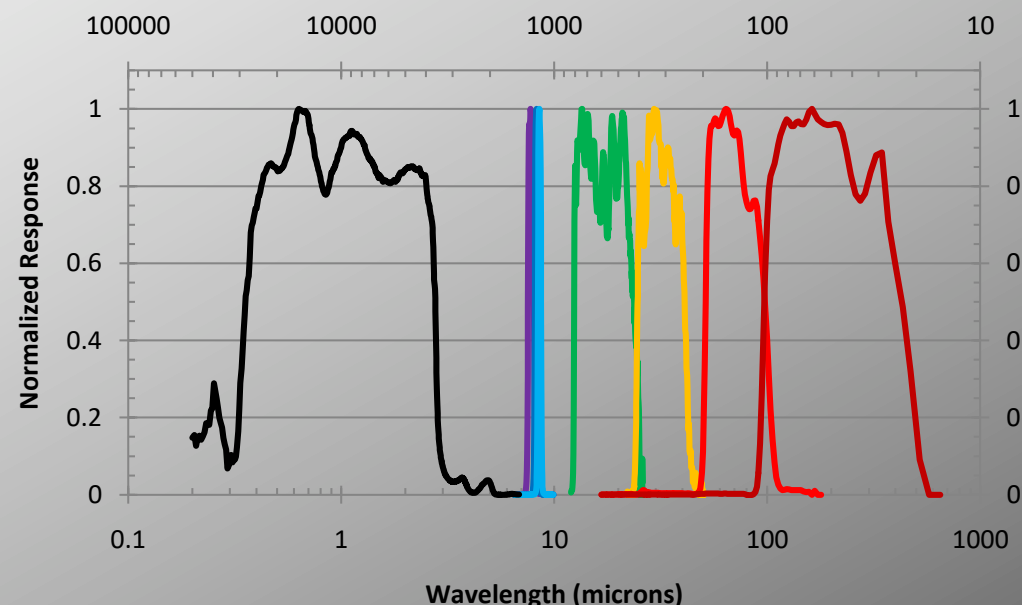
LRO Diviner

UCLA JPL



- Operating in low-altitude lunar orbit since 2009 onboard NASA's Lunar Reconnaissance Orbiter
- Global measurements at ~250-m scale
- Complete local time coverage

Wavenumber (cm⁻¹)



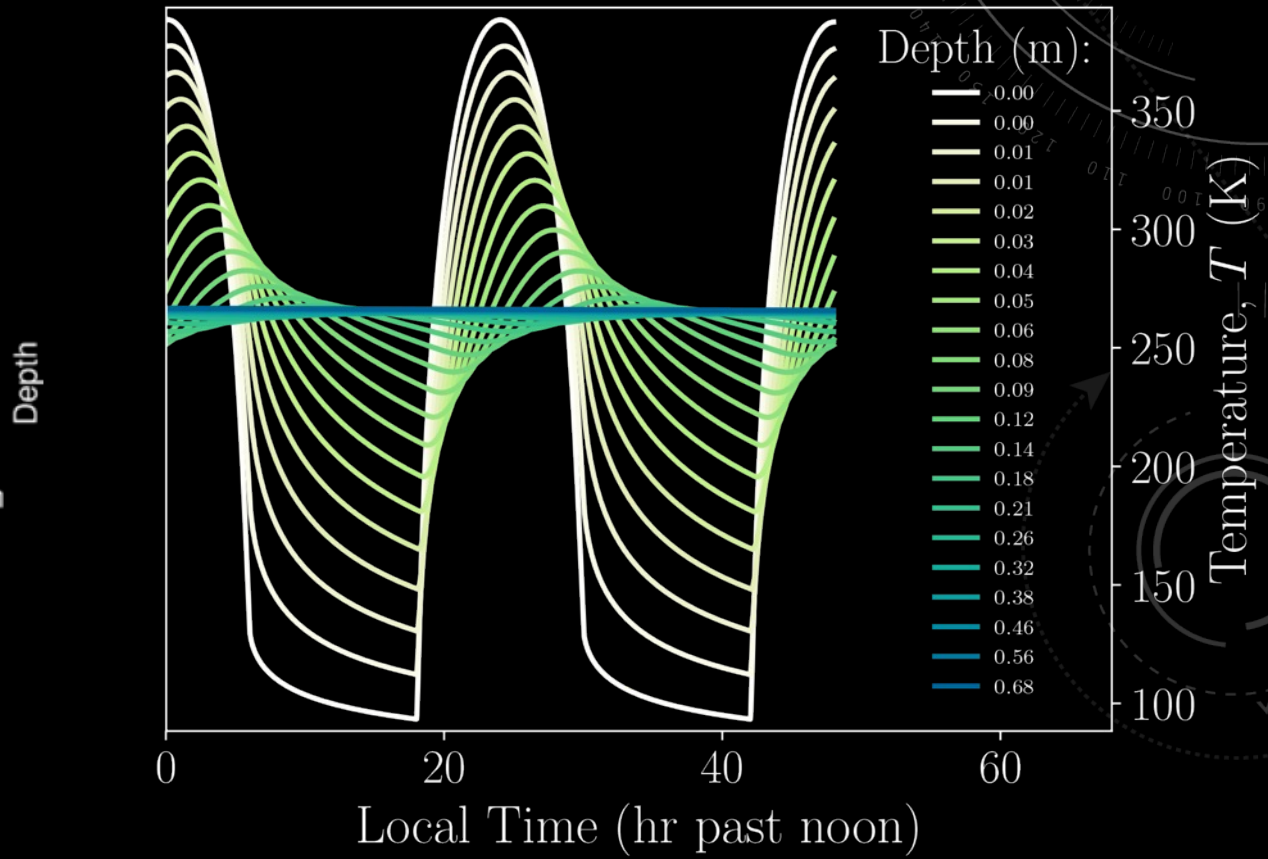
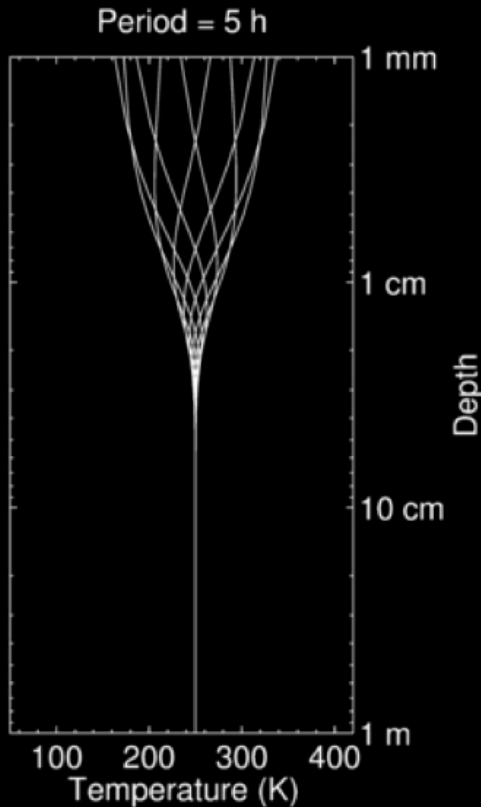
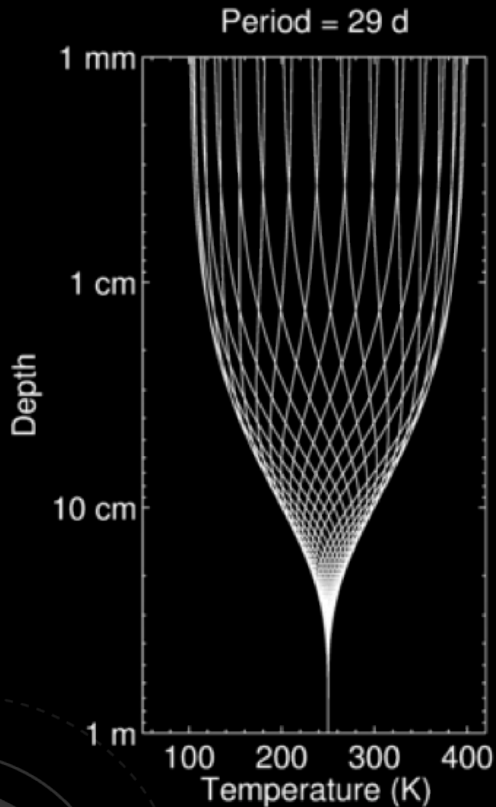
Observation Strategy	Pushbroom mapping, targeted scanning
Detectors	Nine 21-element linear arrays of uncooled thermopile detectors
Fields of view	Detector Geometric IFOV: 6.7 mrad in-track 3.4 mrad cross track 320 m on ground in track for 50 km altitude 160 m on ground cross track for 50 km altitude Swath Width (Center to center of extreme pixels): 67 mrad; 3.4 km on ground for 50 km altitude

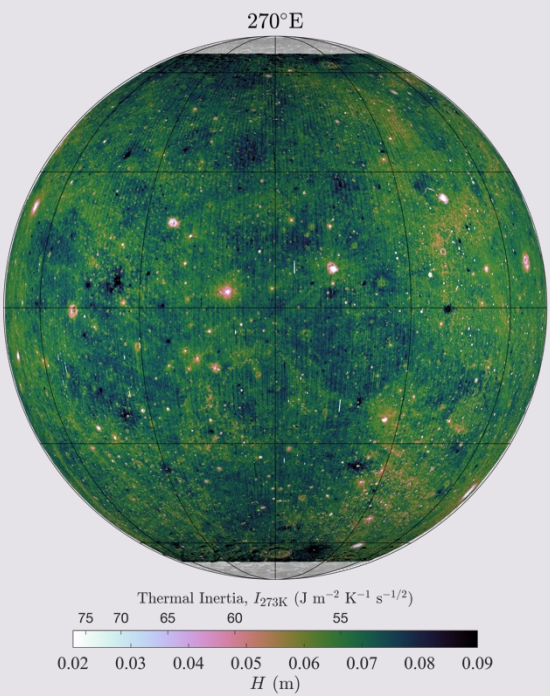
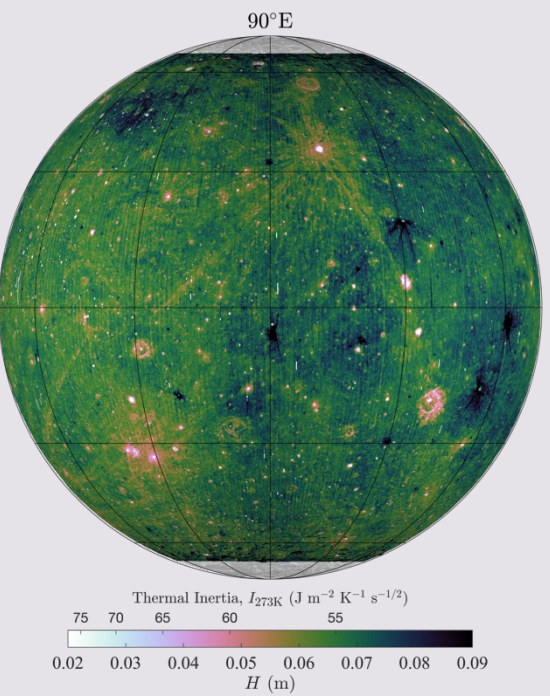
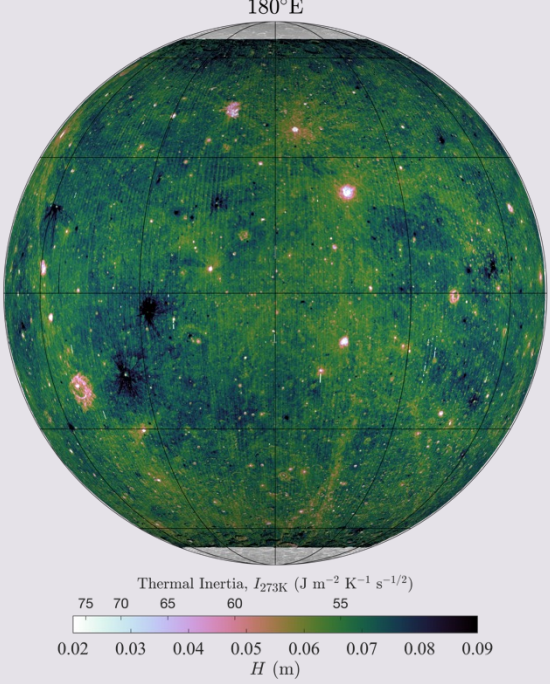
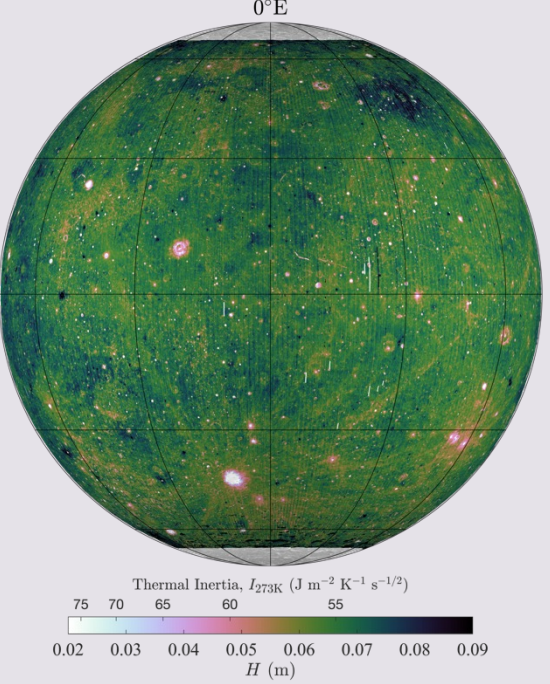
Thermal IR Remote Sensing

A range of sensing depths:

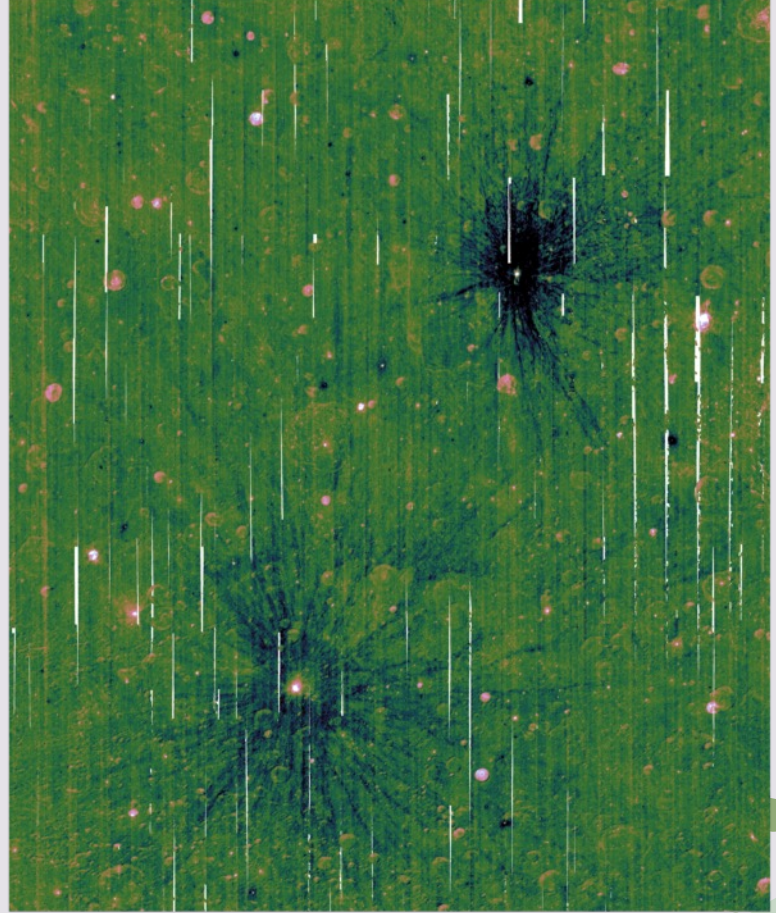
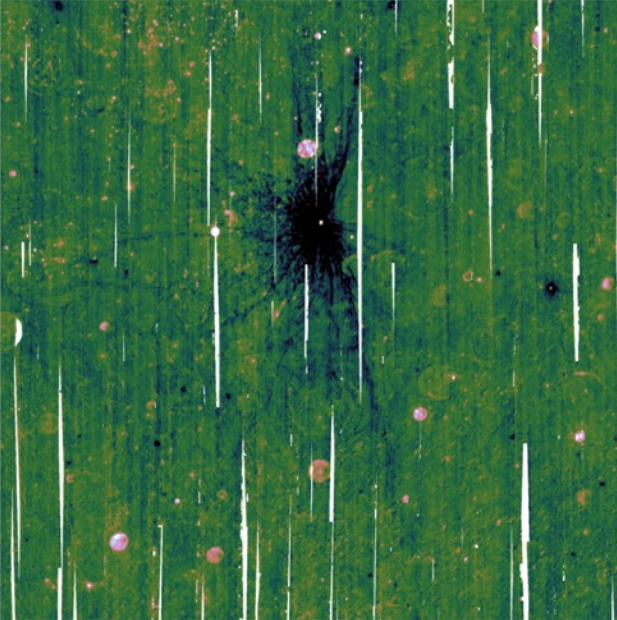
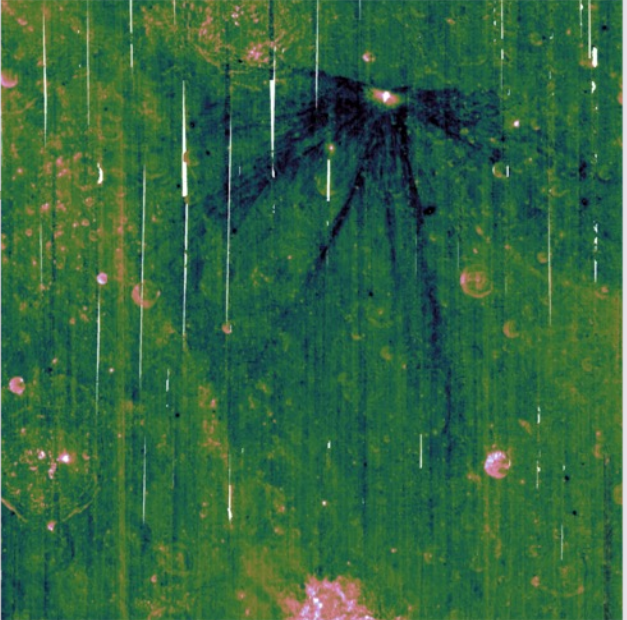
1. Thermal skin depth, $\sqrt{\kappa P/\pi}$
2. Optical skin depth, $(\pi r^2 Q_{\text{ext}} n)^{-1}$

$\sim 10 \text{ cm}$
 $\sim 0.1 \text{ mm}$





Cold Spots

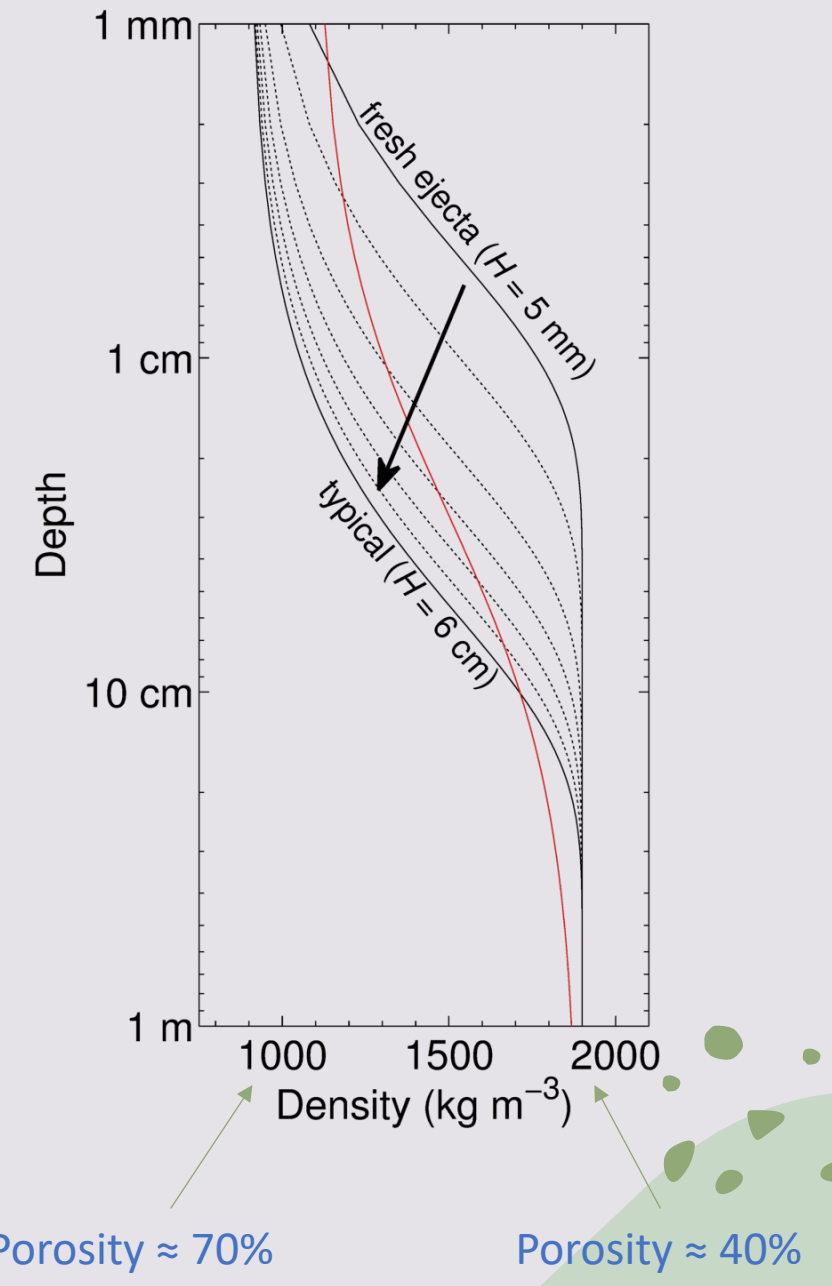
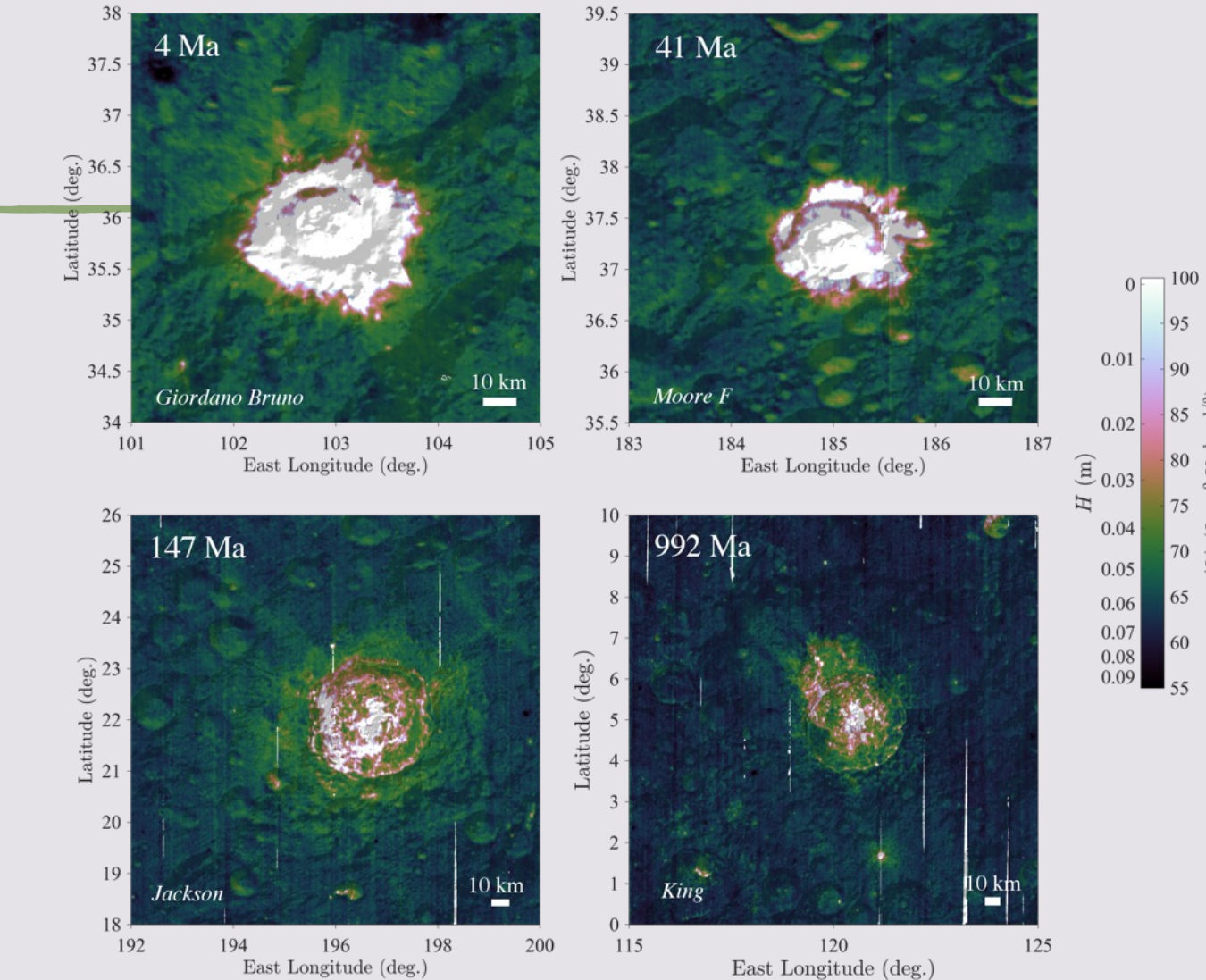


Numerous low-thermal inertia anomalies, range in size from < 1 km to >100 km

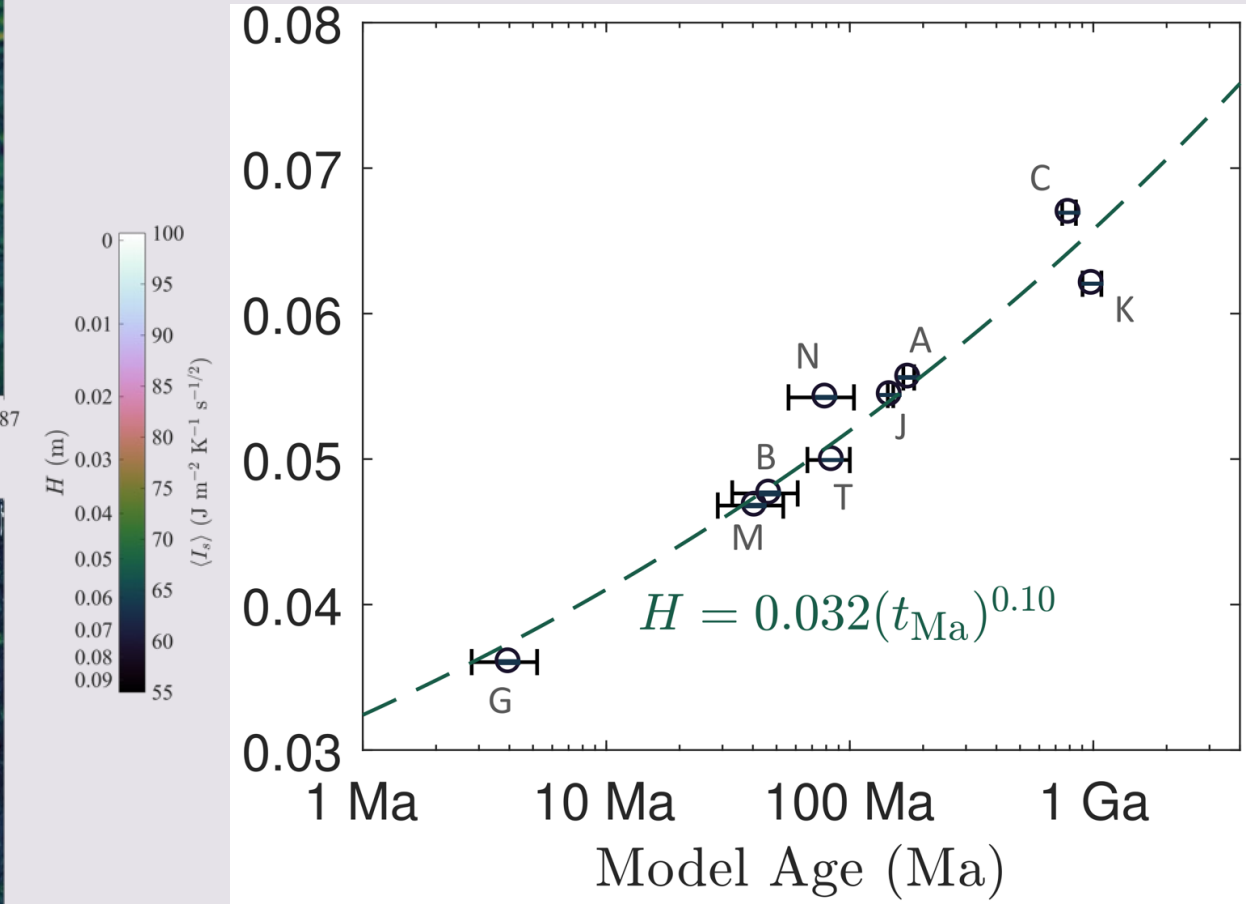
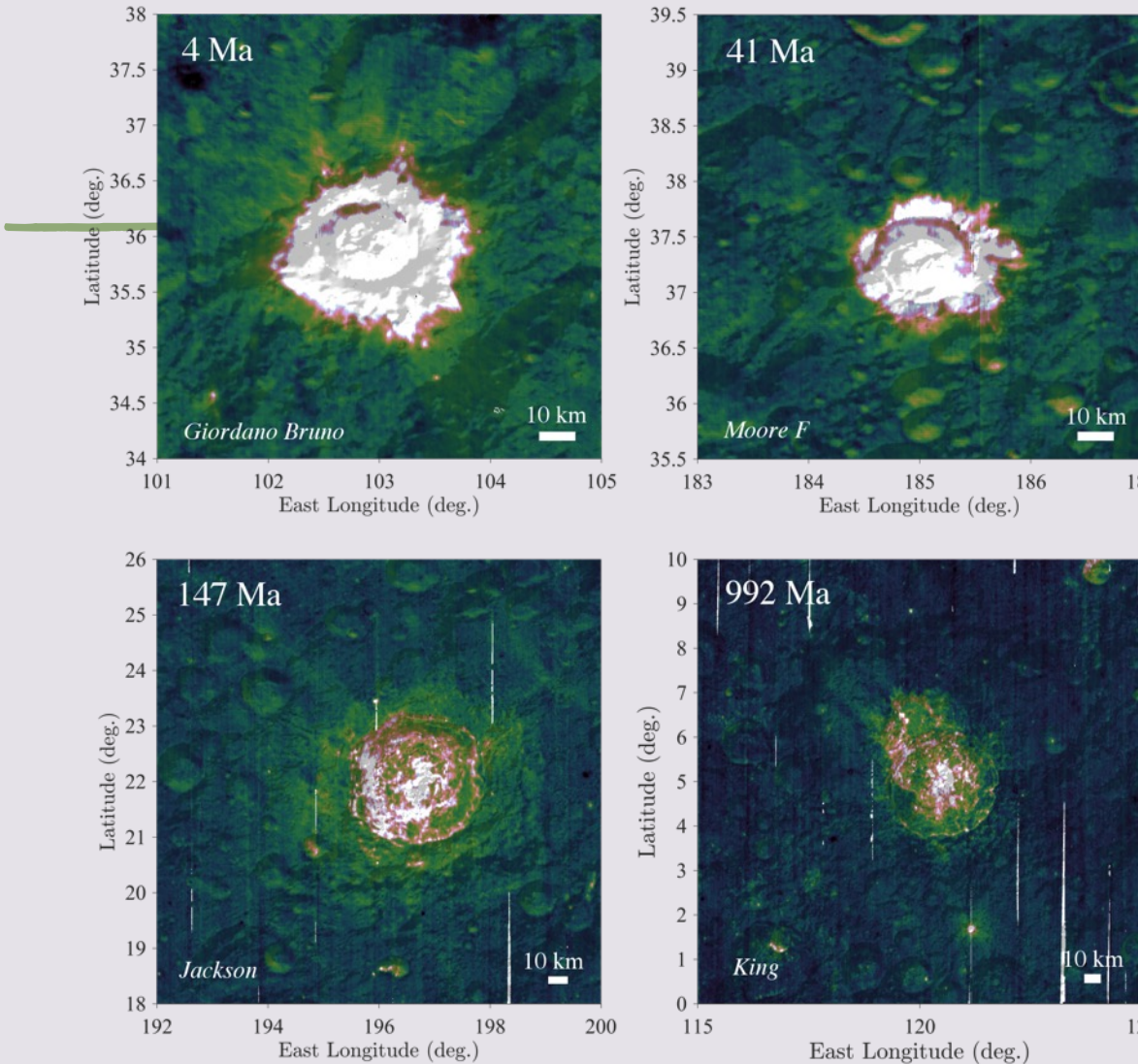
Average age ~ 100 kyr based on population statistics

Formation and fading mechanisms unknown

Regolith Formation



Copernican Craters



Total Lunar Eclipse of 2018 Jan 31

Ecliptic Conjunction = 13:27:53.0 TD (= 13:26:42.5 UT)

Greatest Eclipse = 13:31:00.1 TD (= 13:29:49.6 UT)

Penumbral Magnitude = 2.2941 P. Radius = 1.2978° Gamma = -0.3014

Umbral Magnitude = 1.3155 U. Radius = 0.7567° Axis = 0.3058 $^{\circ}$

Saros Series = 124 Member = 49 of 74

Sun at Greatest Eclipse (Geocentric Coordinates)

R.A. = 20h56m18.8s

Dec. = $-17^{\circ}17'46.9''$

S.D. = $00^{\circ}16'14.0''$

H.P. = $00^{\circ}00'08.9''$

N
Earth's Penumbra

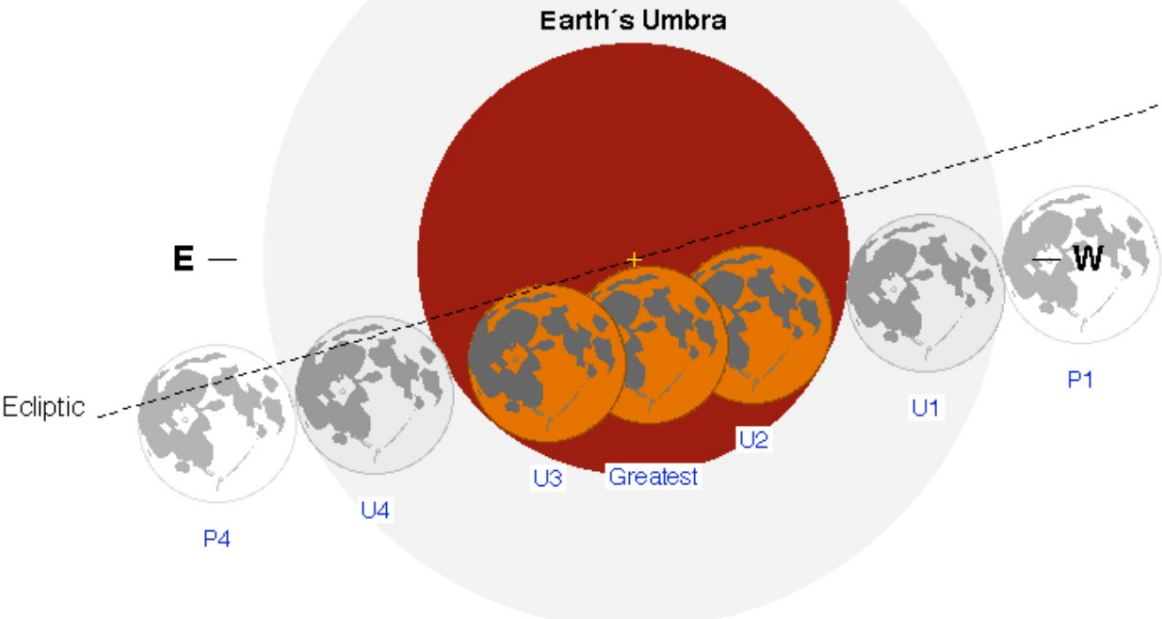
Moon at Greatest Eclipse (Geocentric Coordinates)

R.A. = 08h56m05.0s

Dec. = $+16^{\circ}59'44.1''$

S.D. = $00^{\circ}16'35.2''$

H.P. = $01^{\circ}00'52.5''$



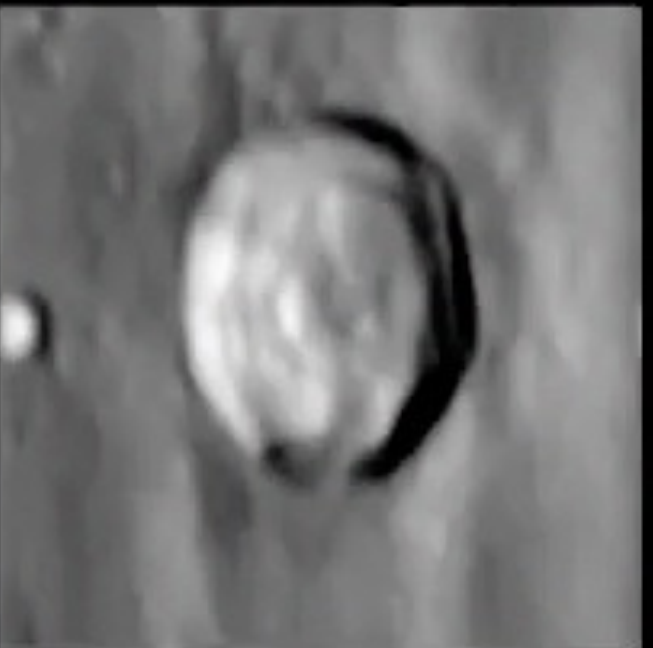
AEOS: Advanced Electro Optomechanical System

- Owned and operated by US Air Force on Haleakala, Maui
- 3.7-m primary mirror, fully articulated mount
- Multiple instruments, including long-wave infrared imager (LWIR) w/ ~1 km/px resolution on Moon



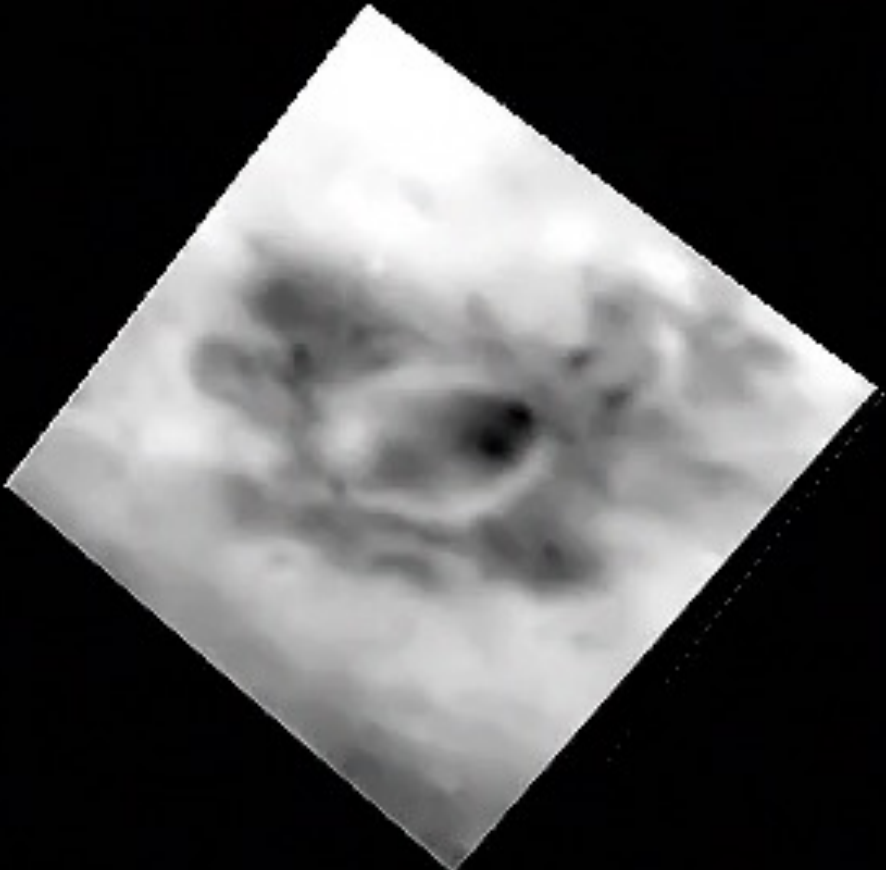
AEOS Data

Kepler Crater



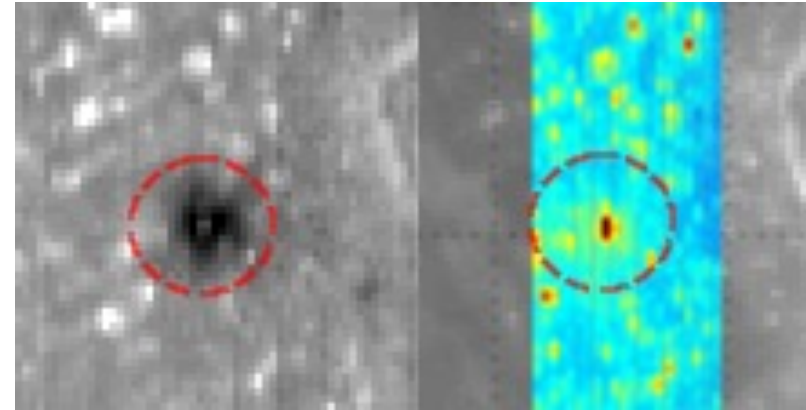
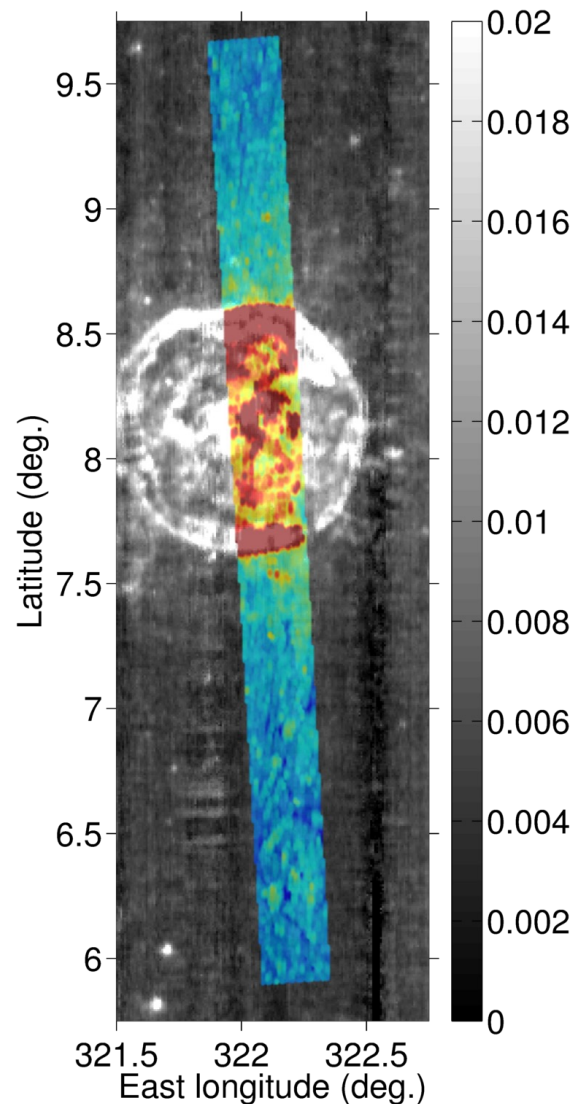
AEOS Data

Reiner Gamma (lunar “swirl”)



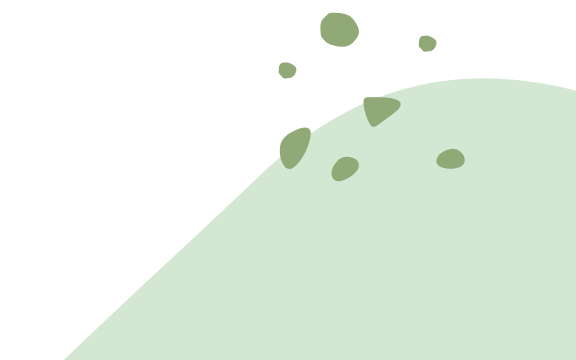
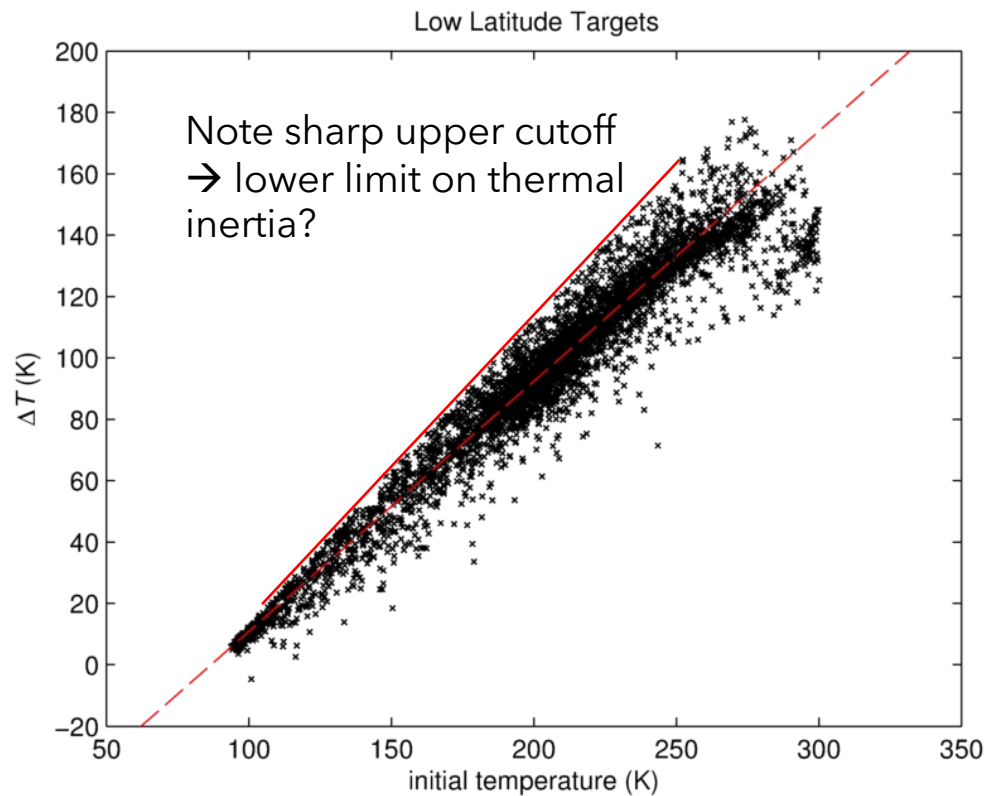
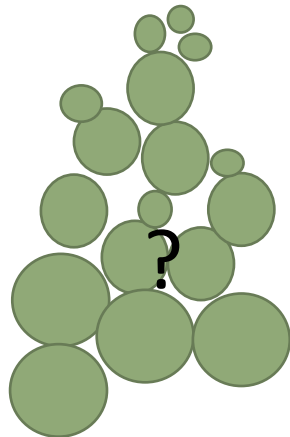
Small Rocks and Cold Spots

Colors = Eclipse cooling

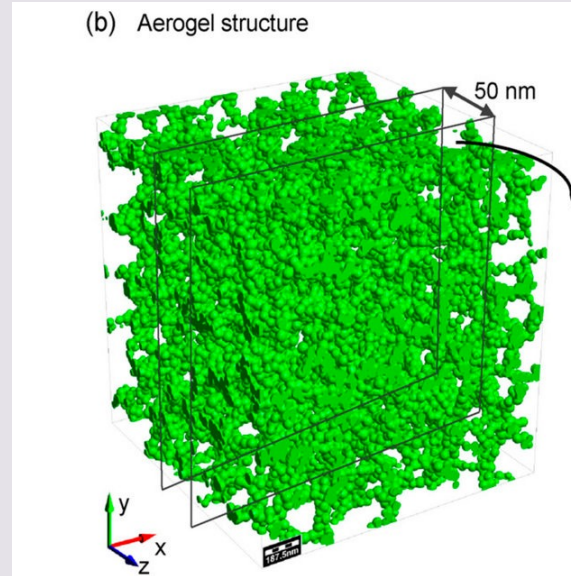
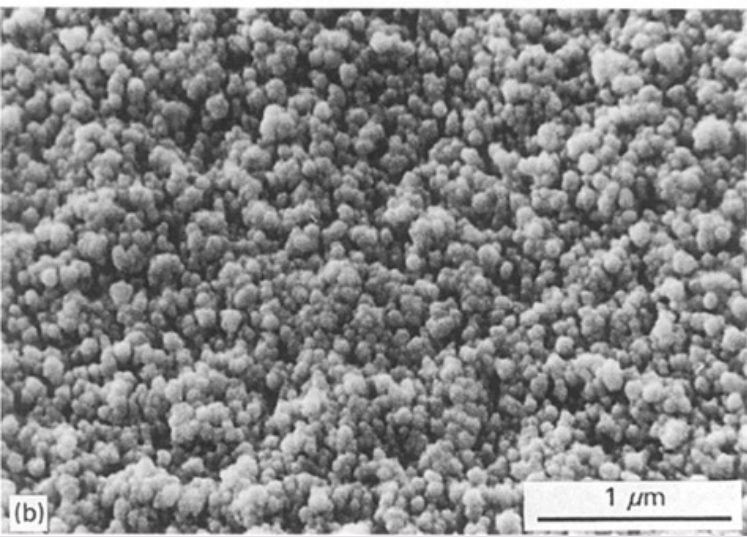


- Smaller rocks detected in eclipse data as spatially extensive warm regions around craters
- Cold spots are actually warmer than surrounding surfaces during eclipse
 - Probably indicates removal of the "epiregolith" by ballistic sedimentation

Appearance of the Epiregolith in Eclipse Cooling

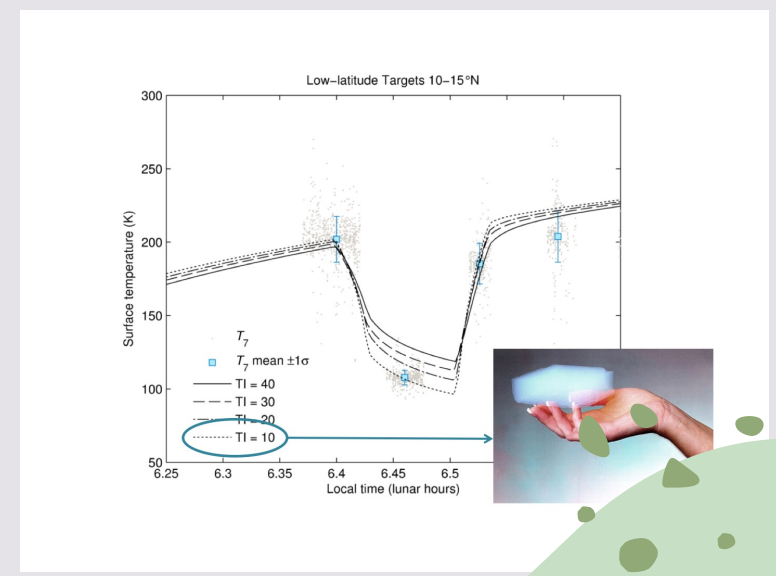


Natural Limit on Conductivity?



Thermal inertia of $10 \text{ J m}^{-2} \text{ K}^{-1} \text{ s}^{1/2}$ of upper ~1 cm regolith derived from eclipse cooling similar to silica aerogel: synthetic material with >90% porosity

Is this the “fairy castle” structure?



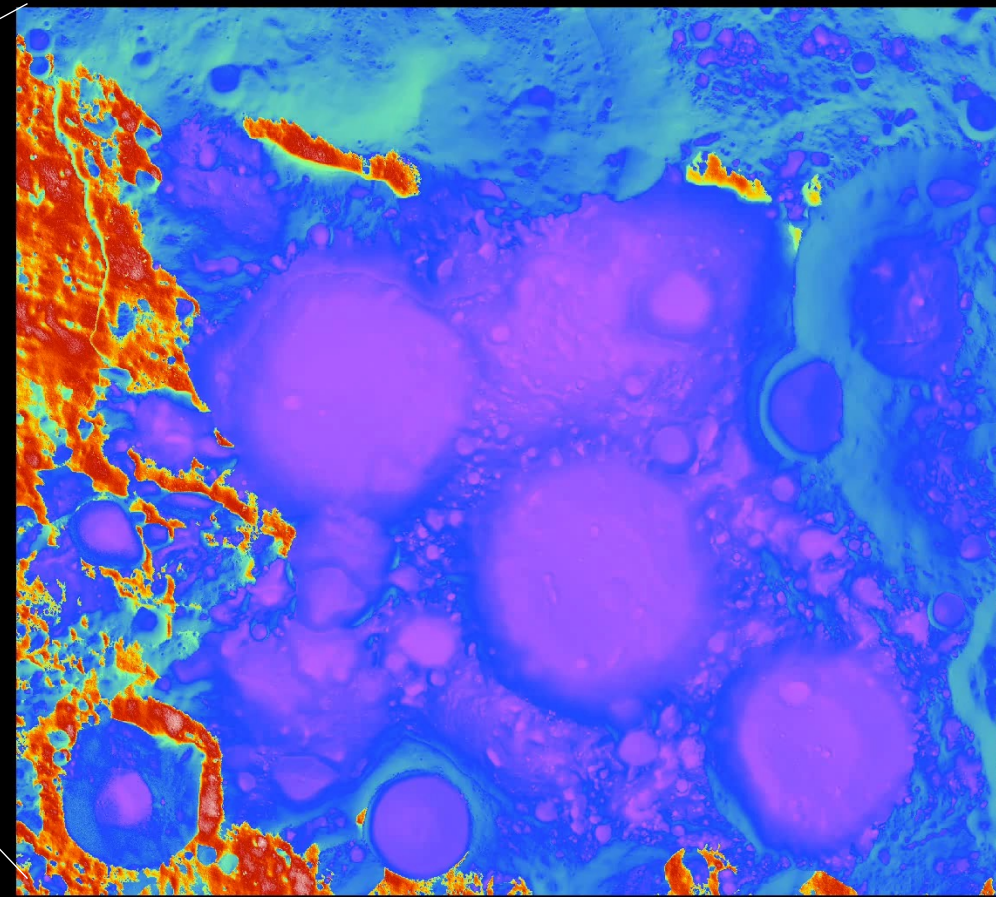
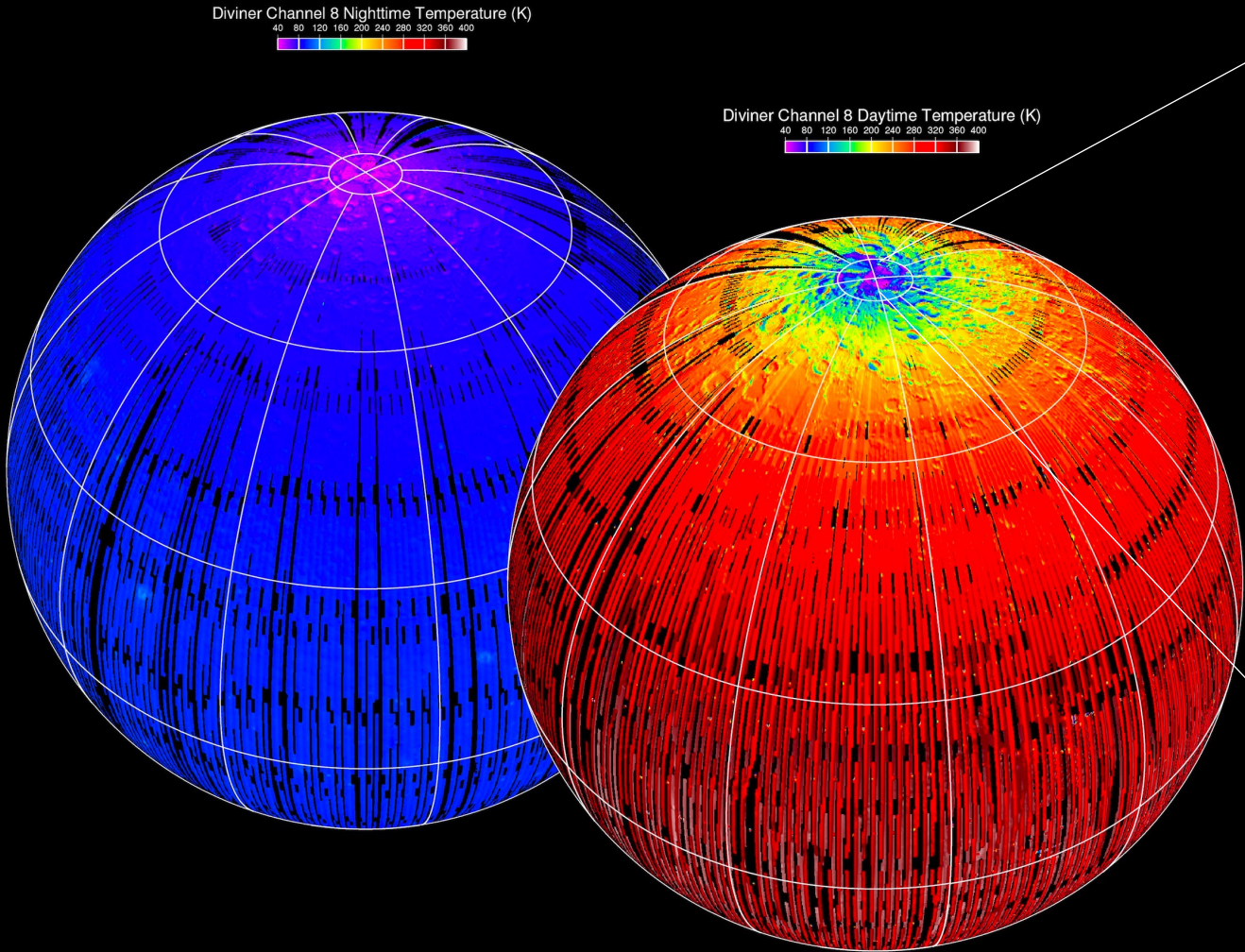
New Views from the Lunar Reconnaissance Orbiter Era

2. Volatiles



Polar Temperatures

Coldest place in the solar system: < 40 K



LCROSS Centaur impact site, Cabeus crater

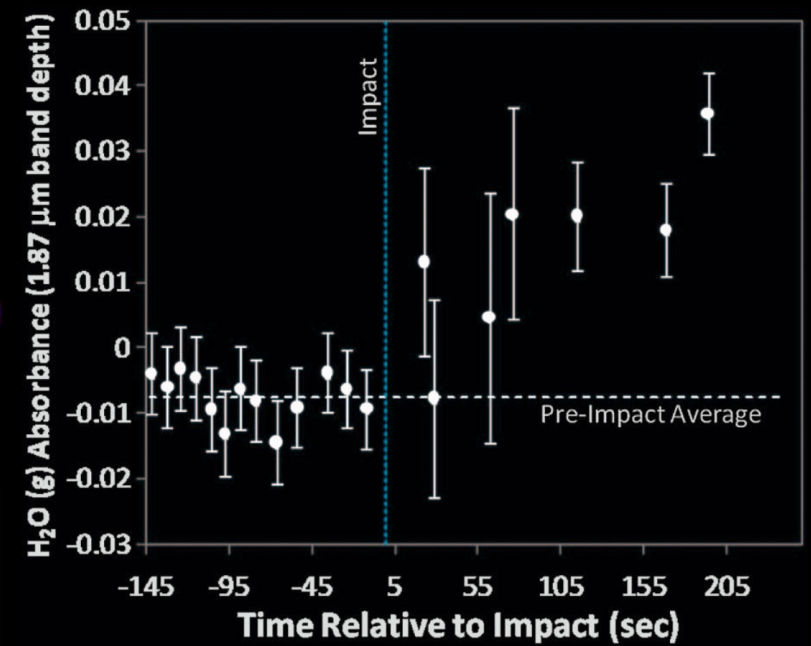
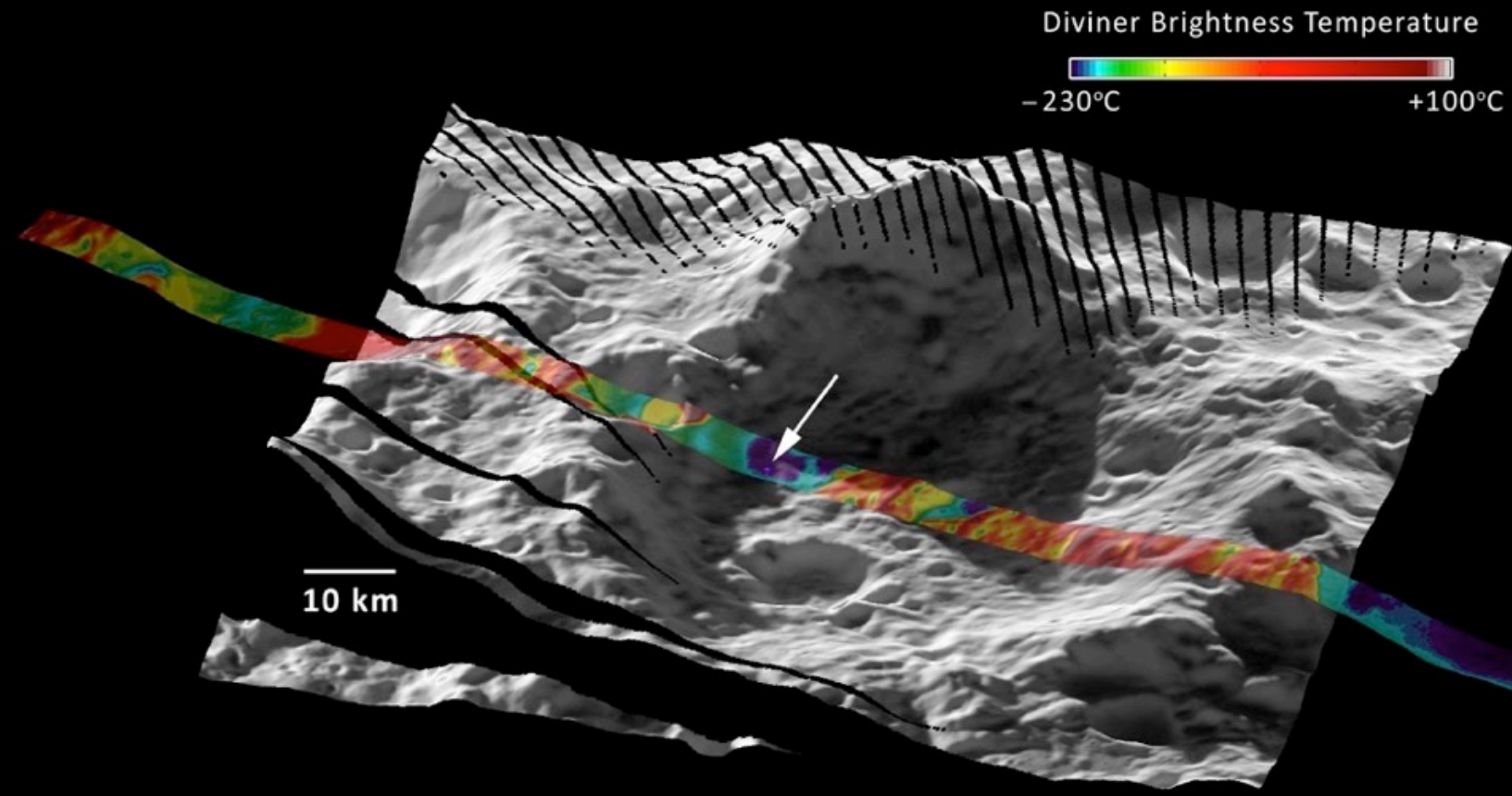
Modeled annual mean temperature
(approx. view from LRO)

78 km slant range
48° emission

LRO

LRO Observes LCROSS





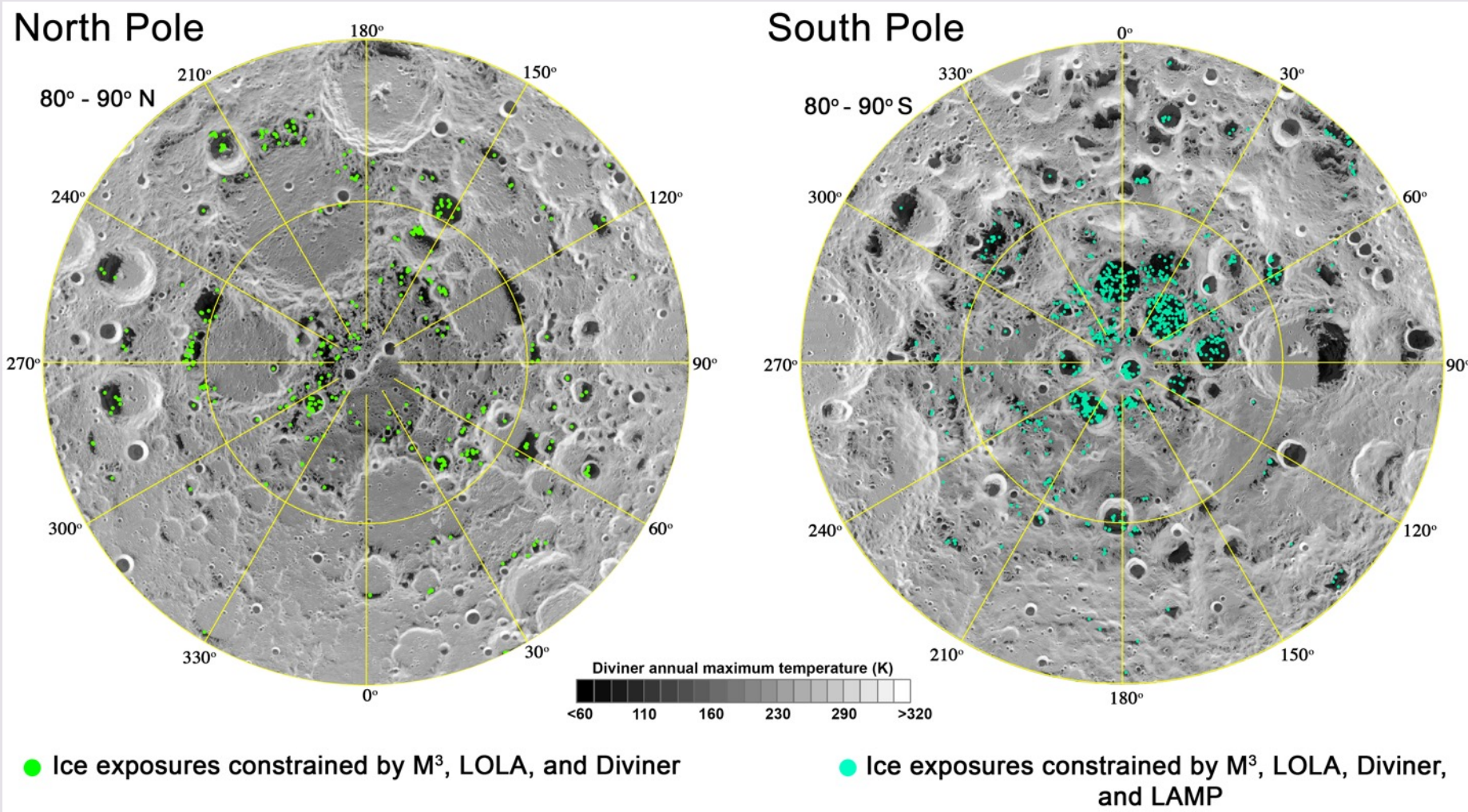
LCROSS results: ~5-7% H₂O ice

Models correctly predicted: H₂S, CO₂, SO₂, NH₃, CH₃OH

Models missed: CH₄, H₂

(Colaprete et al., 2010; Paige et al., 2010; Hayne et al., 2010)

Signatures of Exposed Surface Ice



Up to 30% ice in some locations

Hayne et al. (2015); Fisher et al. (2017); Li et al. (2018)

“Patchiness” of Lunar Ice and the Exosphere Problem

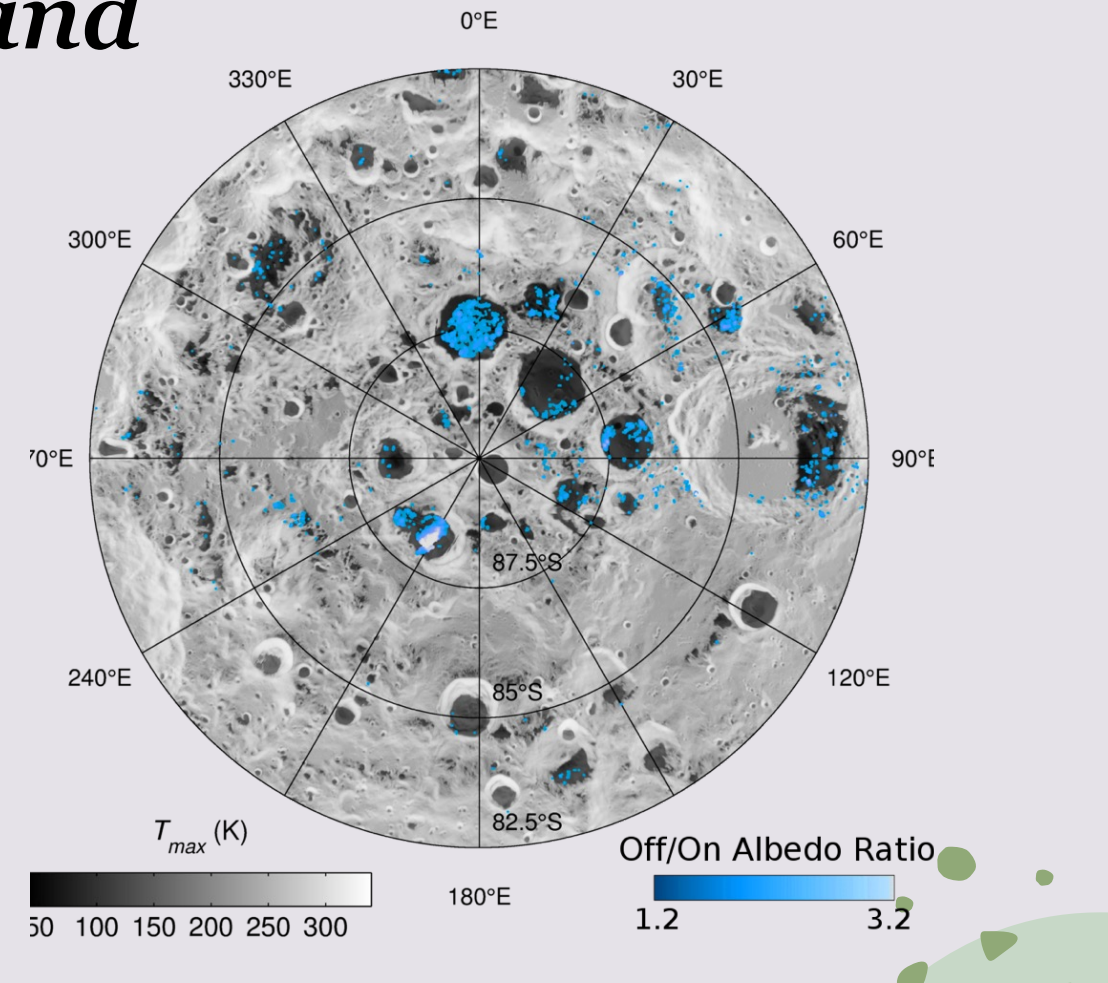
Heterogeneity unexpected if supply > destruction rate

Implies anisotropy in source or loss process

Suggests supply and destruction of water on the Moon may be close to equilibrium

Problems with WMB model:

- No significant background water detected in the exosphere (Benna et al., 2019)
- Diurnal cycle of argon implies empty bonding sites on lunar surface grains; water should occupy these (Hodges, 2002)

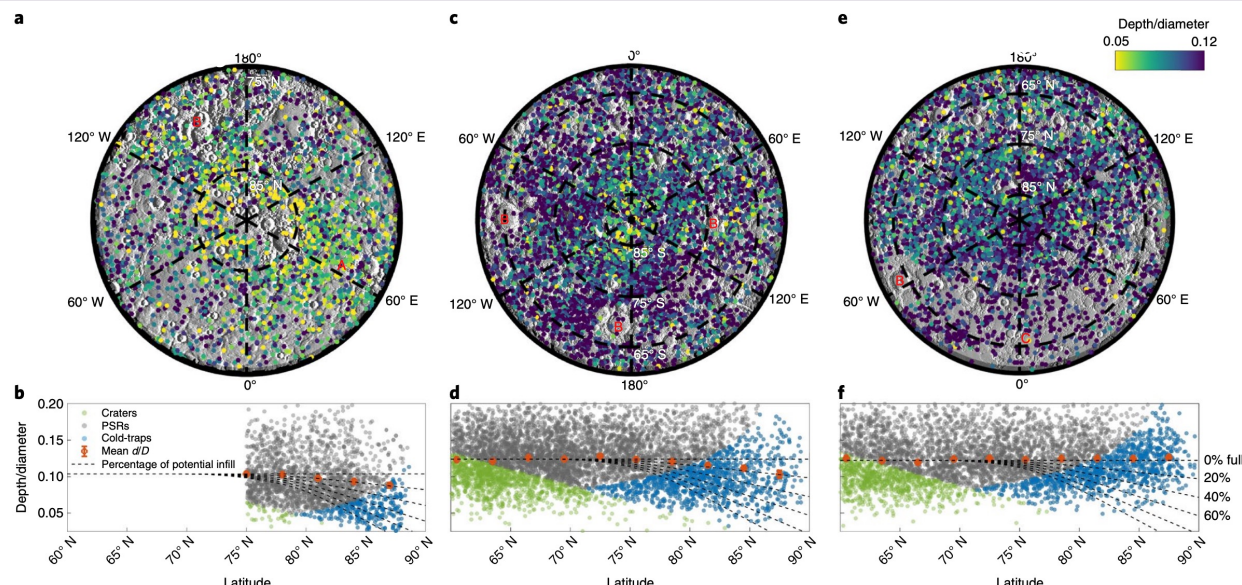


Hayne et al. (2015)

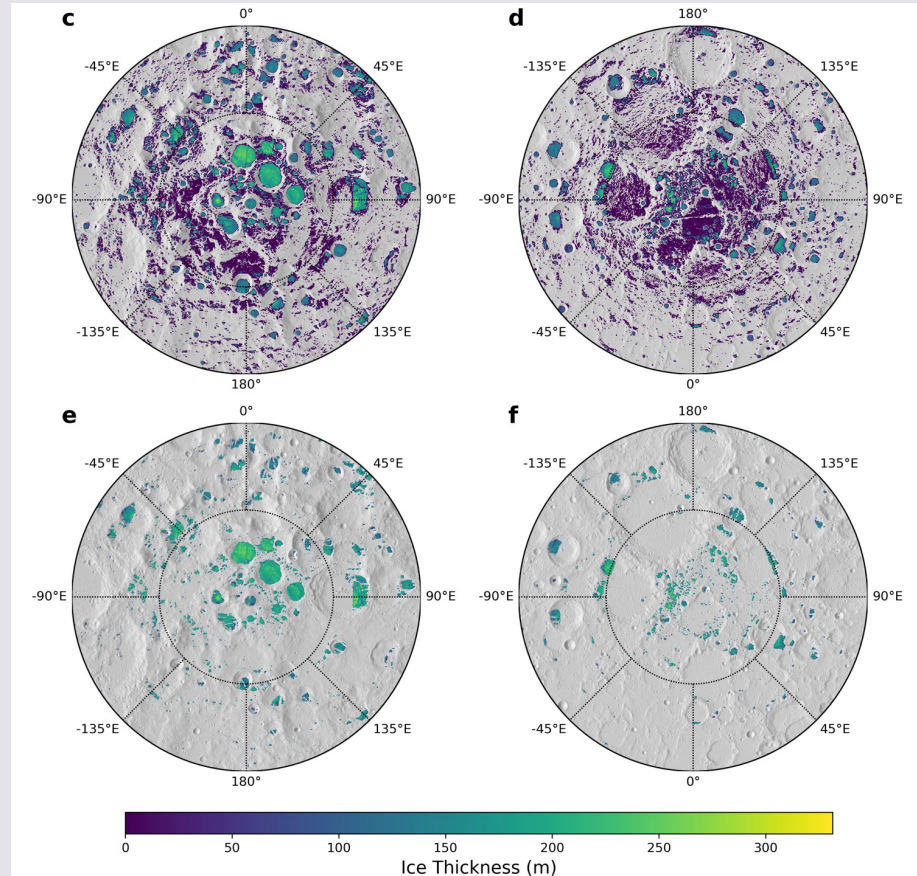
Thick ice deposits in shallow simple craters on the Moon and Mercury

Lior Rubanenko *, Jaahnavee Venkatraman and David A. Paige

Permanently shadowed regions near the poles of Mercury and the Moon may cold-trap water ice for geologic time periods. In past studies, thick ice deposits have been detected on Mercury, but not on the Moon, despite their similar thermal environments. Here we report evidence for thick ice deposits inside permanently shadowed simple craters on both Mercury and the Moon. We measure the depth/diameter ratio of approximately 2,000 simple craters near the north pole of Mercury using Mercury Laser Altimeter data. We find that these craters become distinctly shallower at higher latitudes, where ice is known to have accumulated on their floors. This shallowing corresponds to a maximum infill of around 50 m, consistent with previous estimates. A parallel investigation of approximately 12,000 lunar craters using Lunar Reconnaissance Orbiter data reveals a similar morphological trend near the south pole of the Moon, which we conclude is also due to the presence of thick ice deposits. We find that previously detected surface ice deposits in the south polar region of the Moon are spatially correlated with shallow craters, indicating that the surface ice may be exhumed or linked to the subsurface via diffusion. The family of lunar craters that we identify are promising targets for future missions, and may also help resolve the apparent discrepancy between the abundance of frozen volatiles on Mercury and the Moon.



~100-m thick ice deposits from lunar volcanic eruptions



Wilcoski, Hayne, and Landis (2022)

An Alternative Model to WMB

No continuous source of water to the Moon's PSRs

Buried ice results from accumulation during transient collisional atmospheres produced by impacts or volcanism (e.g., Wilcoski et al., 2022)

Surface water detections in the cold traps result from icy ejecta exhumed by impact craters penetrating to the ice table

Impact gardening and burial are stochastic, but isotropic, so temperature controls spatial variations in ice table depth

Once on the surface, ice is rapidly destroyed (Farrell et al., 2019)

Icy Ejecta Model

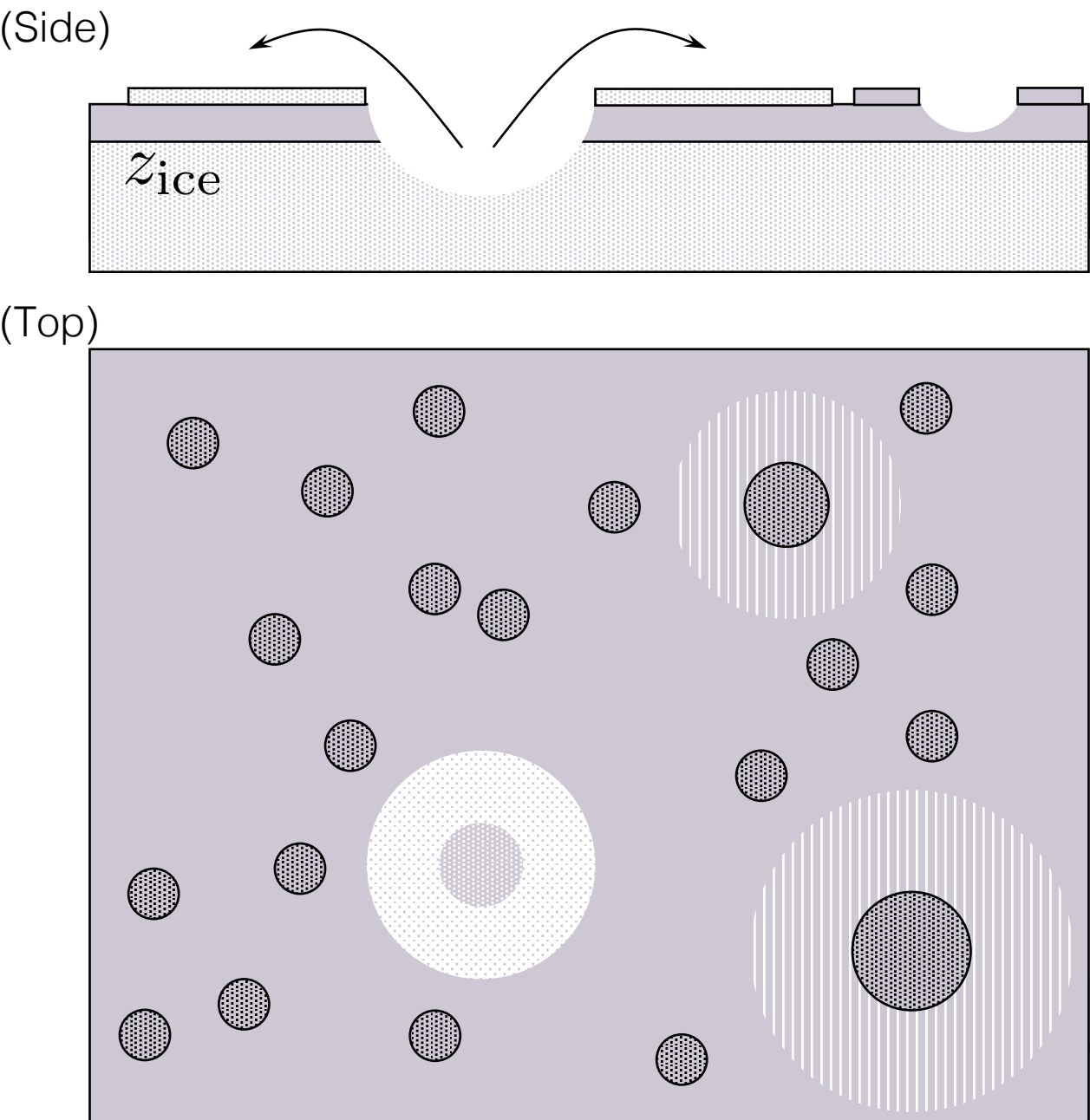
Ice table depth z_{ice} is a discrete boundary at each map location

Craters with transient depths $d > z_{\text{ice}}$ produce icy ejecta

Exposed surface ice is removed on characteristic timescale t_{lifetime}

- Shorter of the sublimation, or non-thermal destruction timescales

Crater production function from Williams et al. (2017)



Icy Ejecta Model

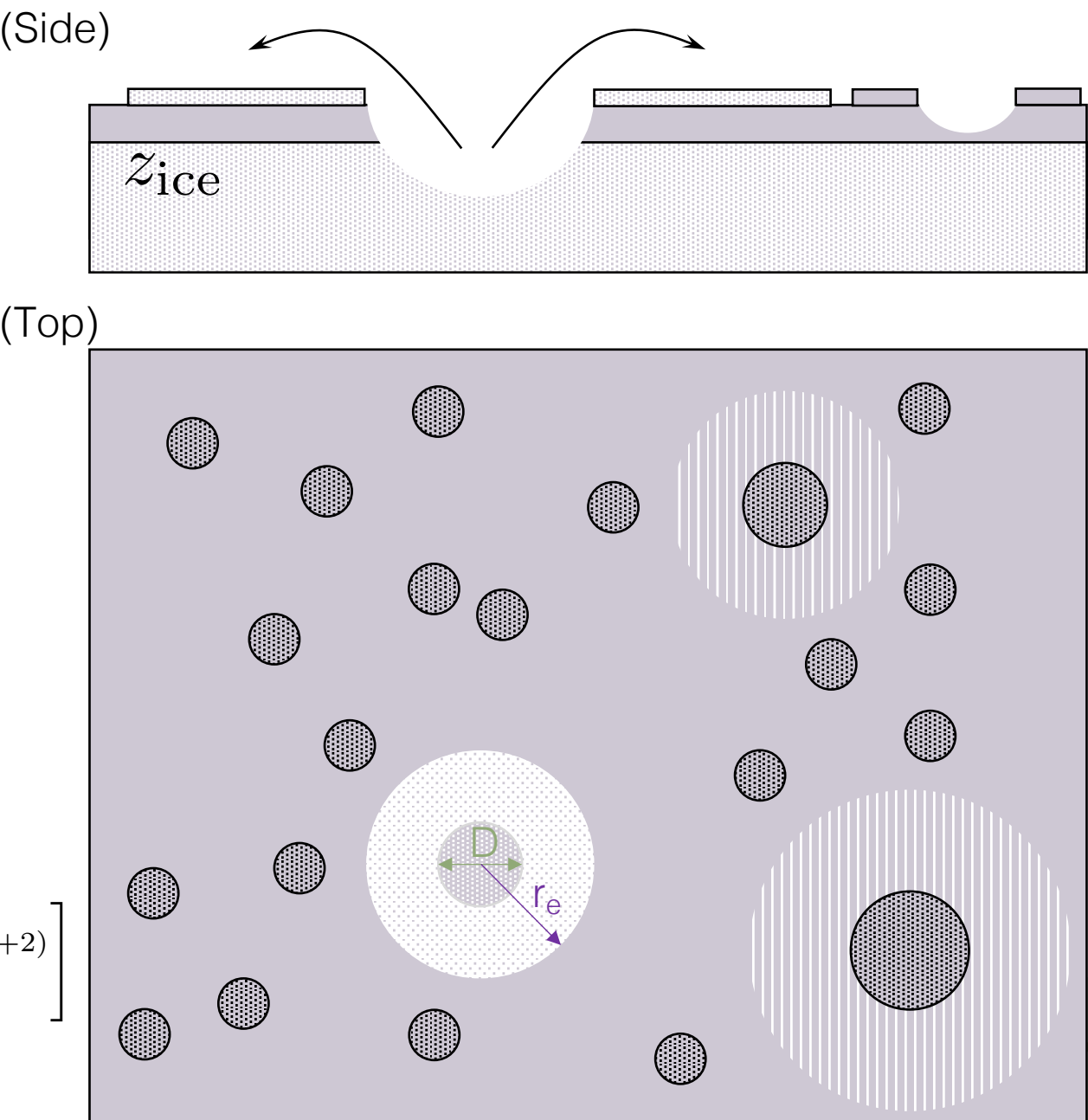
Ejecta radius equal to distance where layer becomes optically thin (Tomlinson and Hayne, 2022):

$$r_e = \frac{D}{2} \left(\frac{h_0}{h_c} \right)^{1/B}$$

Fractional area of ice within a given area during time interval Δt :

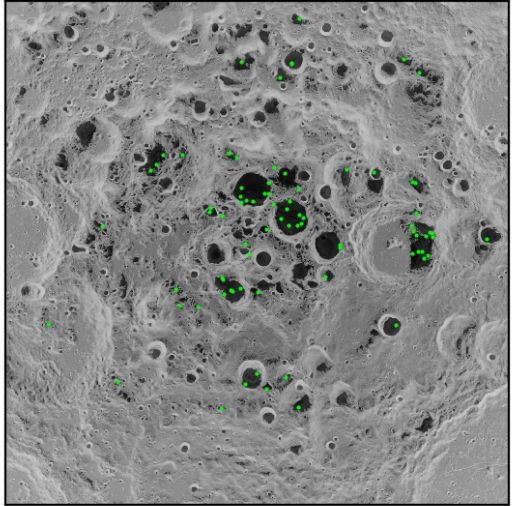
$$f_e(D_0, \Delta t) = \Delta t b C \frac{\pi}{4} \left[\frac{D_0^{(2-b)}}{2-b} - \frac{S}{2/B - b + 2} D_0^{(2/B-b+2)} \right]$$

$$S \equiv \left[\frac{(B-2)\beta}{4h_c} \right]^{2/B}$$

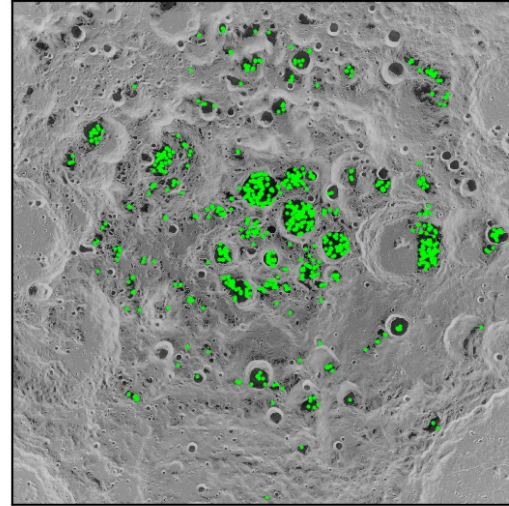


Results

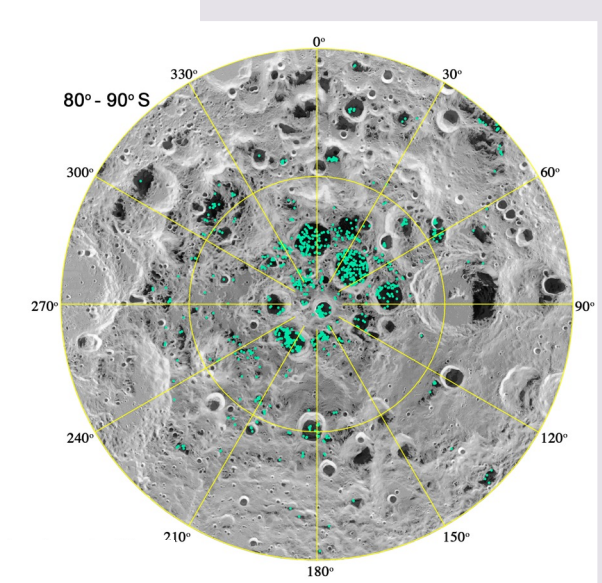
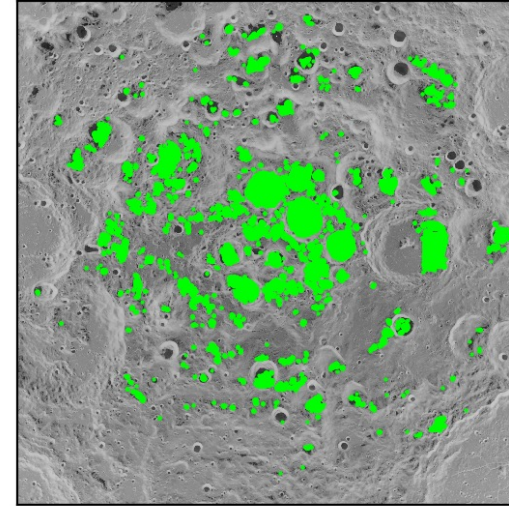
$t_{\text{lifetime}} = 100 \text{ kyr}$



$t_{\text{lifetime}} = 1 \text{ Myr}$

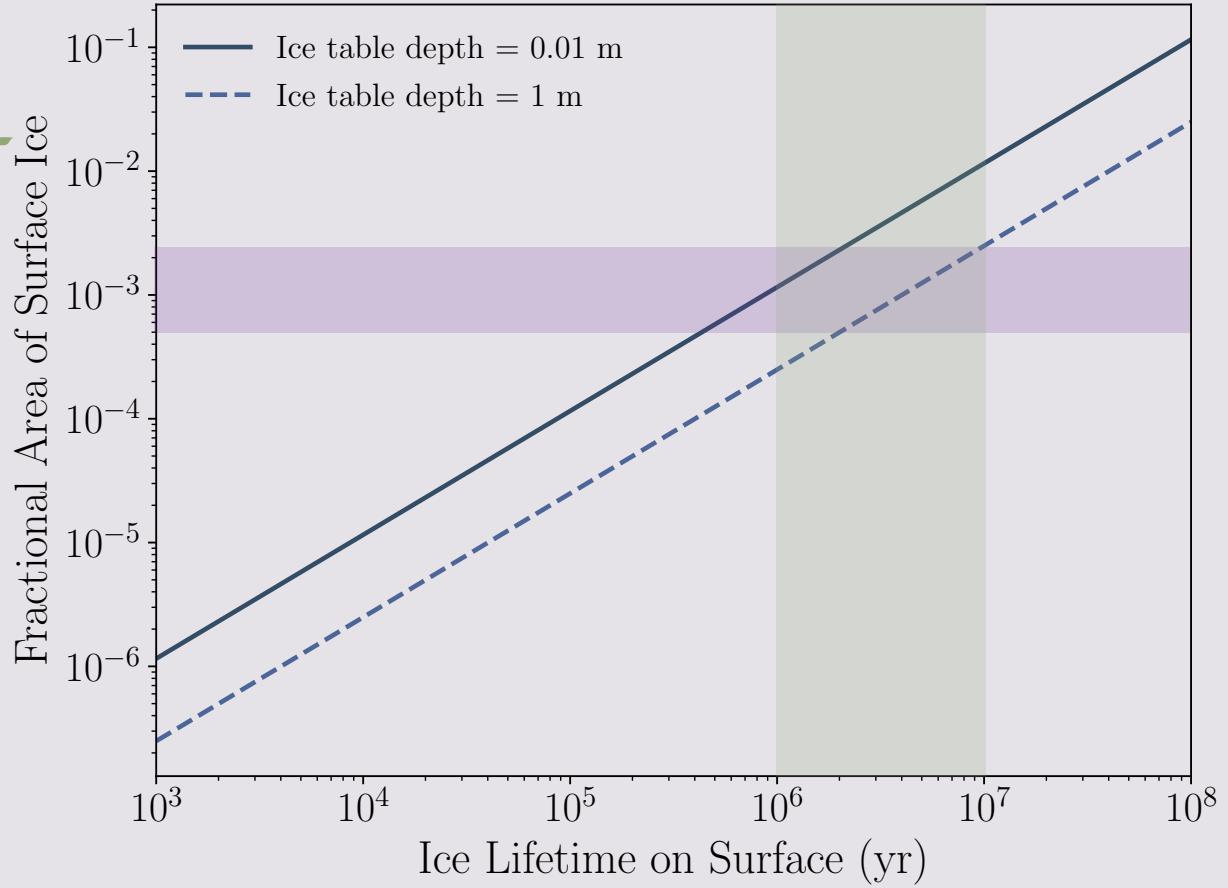


Thermal Loss Only



- Each frame shows a statistically generated pattern of “ice detections” (green dots)
- For each pixel in the map, the likelihood of detection is equal to the fractional area occupied by surface ice for the local thermal conditions and given time interval (surface ice lifetime)
- The map at right from Li et al. (2018) shows ice detections in cyan, which comprise ~0.05% to 0.25% of cold trap area

Results



Purple shaded region shows range of fractional area of positive ice detections from Li et al. (2018)

Timescale for darkening (blue shaded region): $\sim 1\text{-}10$ Myr agrees well with ice detections

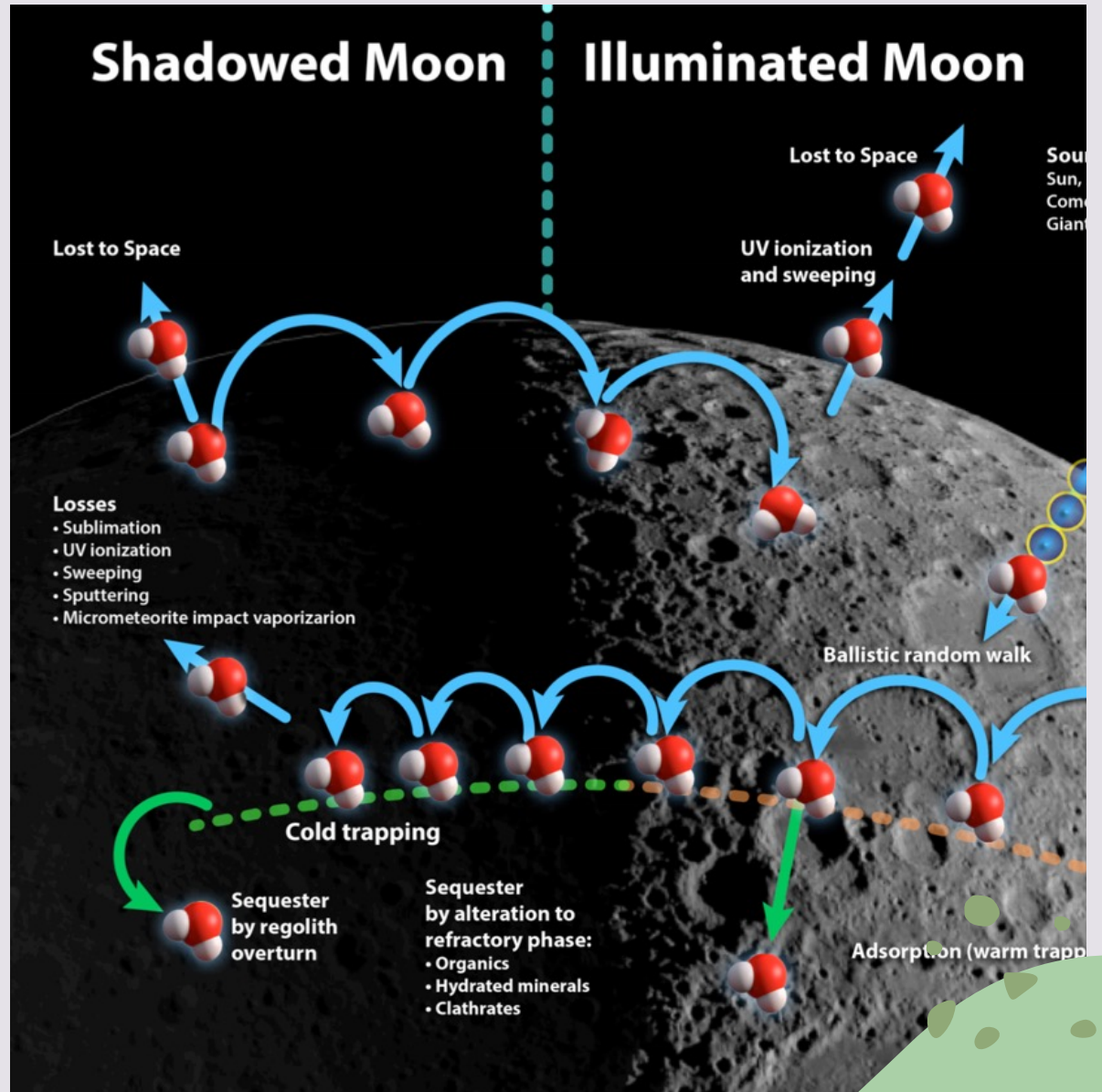
Young Age of Lunar Water

Many more loss processes than source processes

Dominant destruction process on illuminated portion of Moon is photodissociation and escape

Within the cold-traps, water is most rapidly destroyed by impact vaporization and ejection (Farrel et al., 2009)

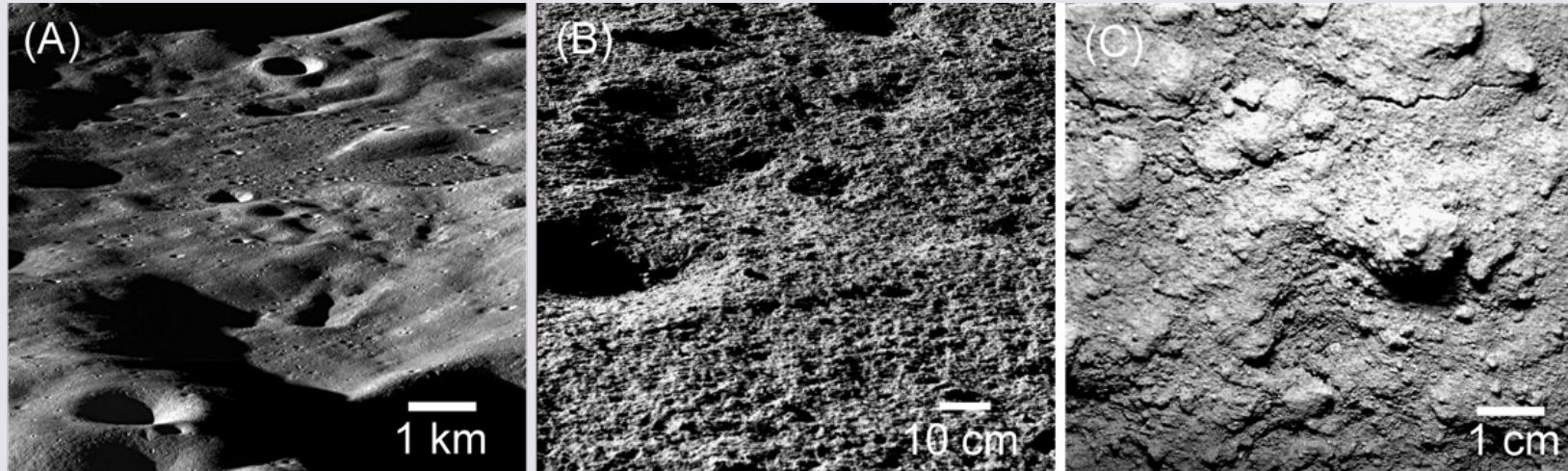
- Observations of surficial water ice imply recent accumulation, possibly < 100 kyr ago



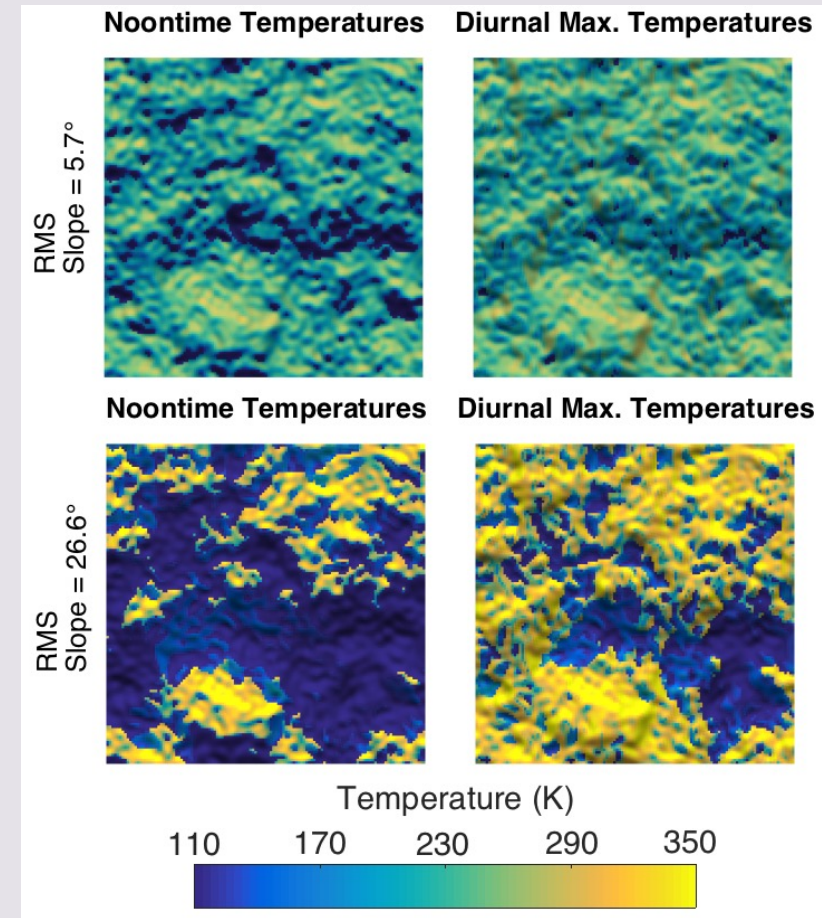


How can we test the hypothesis of a young age for lunar volatiles?

The Case for “Micro Cold Traps”



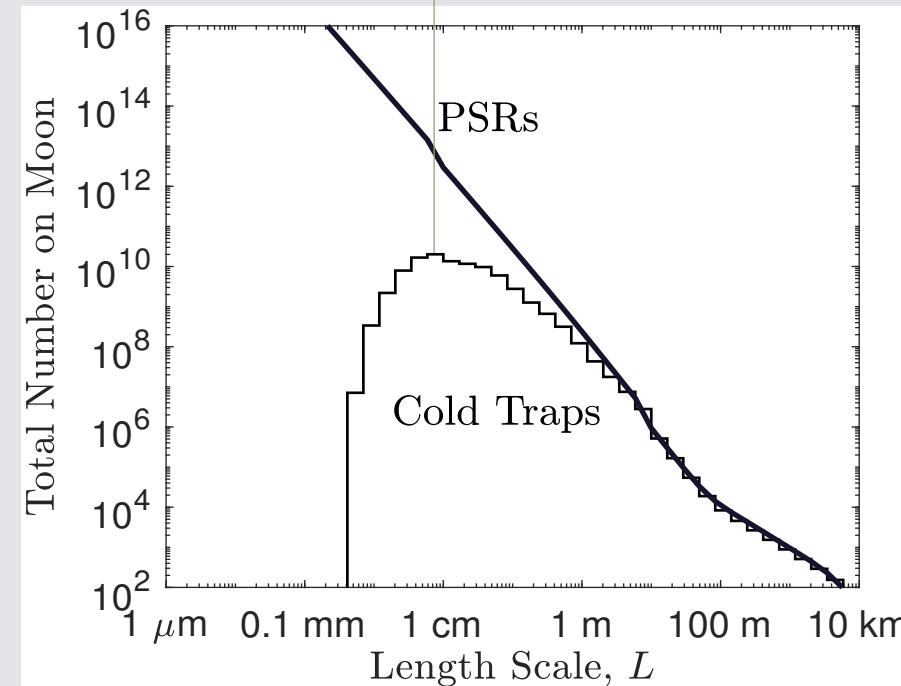
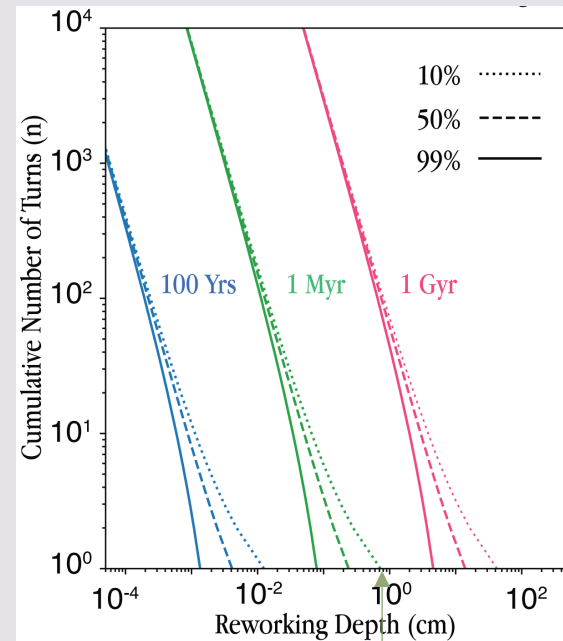
- Enormous temperature gradients: $\sim 100 \text{ K/mm}$ from shadow to sunlight
- Roughness: increases w/ decreasing scale
- *Micro cold traps*: cm-scale shadows could be full of ice if supply rates > gardening rates



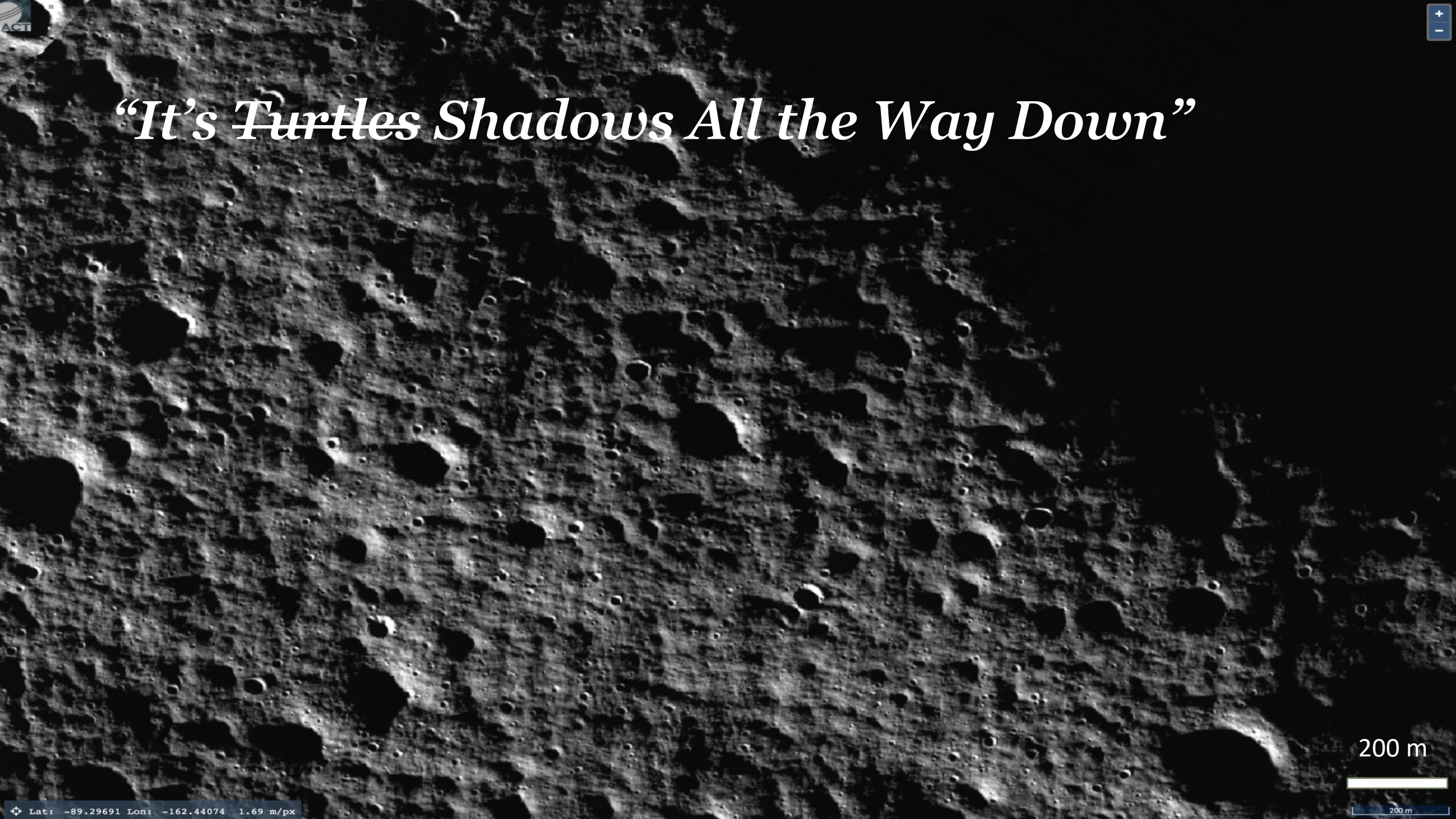
Hayne et al. (2020)

Timescales Revisited

- Shadows < 1 cm are the most numerous on the Moon
- H₂O should be stable for millions of years within the micro cold traps (Costello et al., 2020)
- Micro cold traps are much more accessible than ice in the “deep dark shadows”
- Provides opportunity for robust test of the “young age” hypothesis and exospheric transport



“It’s Turtles Shadows All the Way Down”



200 m

Summary and Looking Ahead

Lunar regolith is remarkably uniform on global scales: < 5% thermal inertia variation (3σ) over the entire Moon

Uppermost ~10 cm has porosity ~70%

Epiregolith within < 1 cm depth has porosity >90%, dominated by fines < 10 μm

Water ice is present in PSRs, but its heterogeneity implies local production/destruction and/or very recent (< 1 Ma) delivery

Moon is still rather dry, as shown by limited exosphere abundance (< 3 cm^{-3}) (Hodges, 2022)

Future measurements from VIPER, CLPS and Artemis will definitively answer the question of whether significant ice deposits exist, and how they got there

VIPER

